The Cosmic Web at High Redshift

Dick Bond, CITA (+ **Kofman, Pogosyan, Wadsley, Myers,..**)

peak-patches: δ > 100, massive galaxies at z - 3

are the rare events in the medium => intermittency

(dwarf galaxies at higher z, groups then clusters at lower z)

filaments: δ ~ 5-10, bridge massive galaxies, dwarfs bead the bridges & there are smaller dwarf bridges

2-peak constraint of nearly-aligned tidal tensors **=> strong bridges**

membranes: δ ~ 2 intrafilament webbing

3,4,...-peak constraint of "clustering patches' of peaks

=> A **"molecular" picture** of large scale structure

Applications of Peak-patch/web ideas

clusters & superclusters: SZ, lens, X-rays at z~.4 (sph/treeP^{3}M)

"reconstruct" initial conditions with "top N" peaks/voids

Y compression of essential LSS info $\{r_{pk}, e_{pk,ij}, V_{pk}, (\nabla \delta_L = 0)\}$

galaxy bias & likelihood of rare super-patches at z ~ 3

peak-patch clustering via multi-box tiling of large regions with phase-coherent ultra-long waves as well as short ones

starbursting galaxies at z ~ 2-4, seen in submm

merging peak-patches

Lyman " forest at z ~ 2-5, filaments + dG's (sph/treeP^{3}M)

"shearing patches", constrained by $\{\langle e_{ij} \rangle_V\} \rightarrow \{\nu, e_v, p_v\}$,

linear tidal field = linear strain field = linear shear field

First Objects: inhomogeneous reionization at z ~ 10-20

Stromgren spheres around 'dwarflet' peak-patch clusters

Las Companas Redshift Survey.

Biggest to date

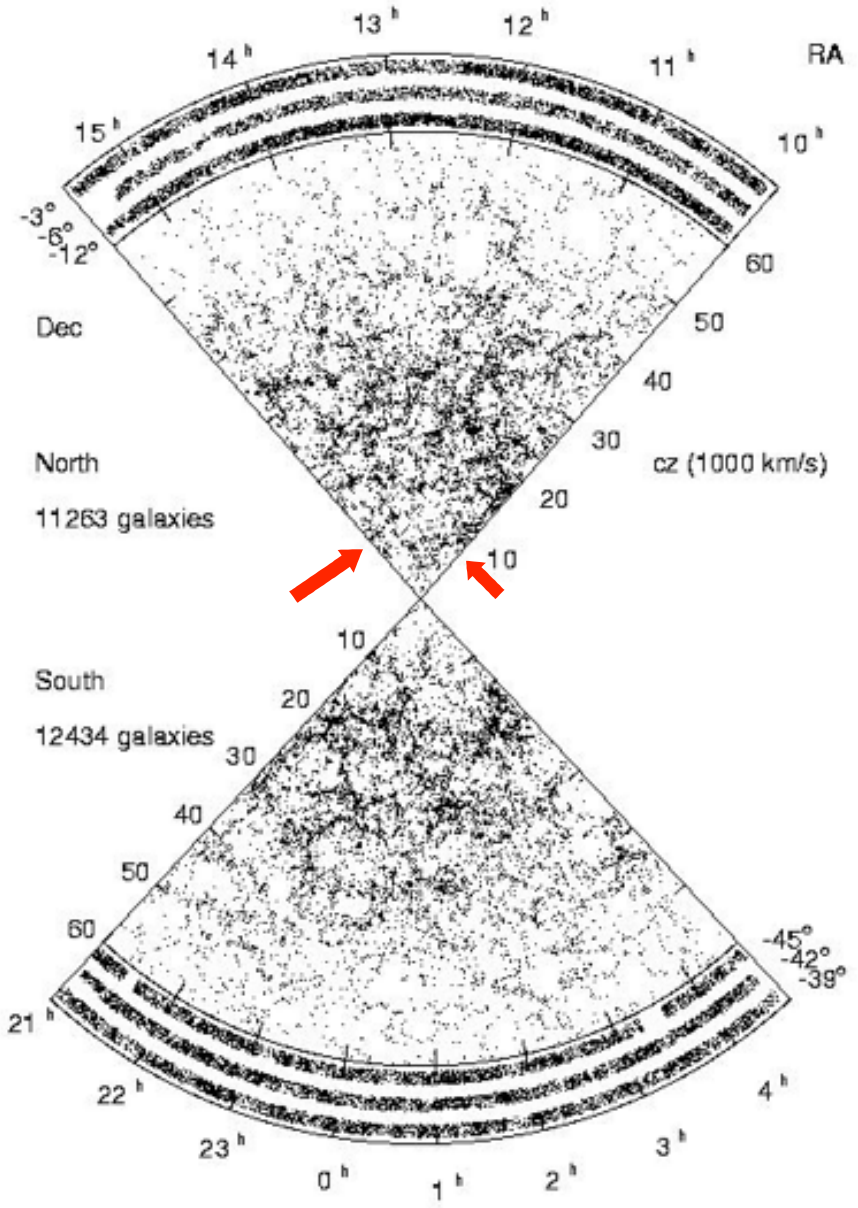

Schectman *et al*.

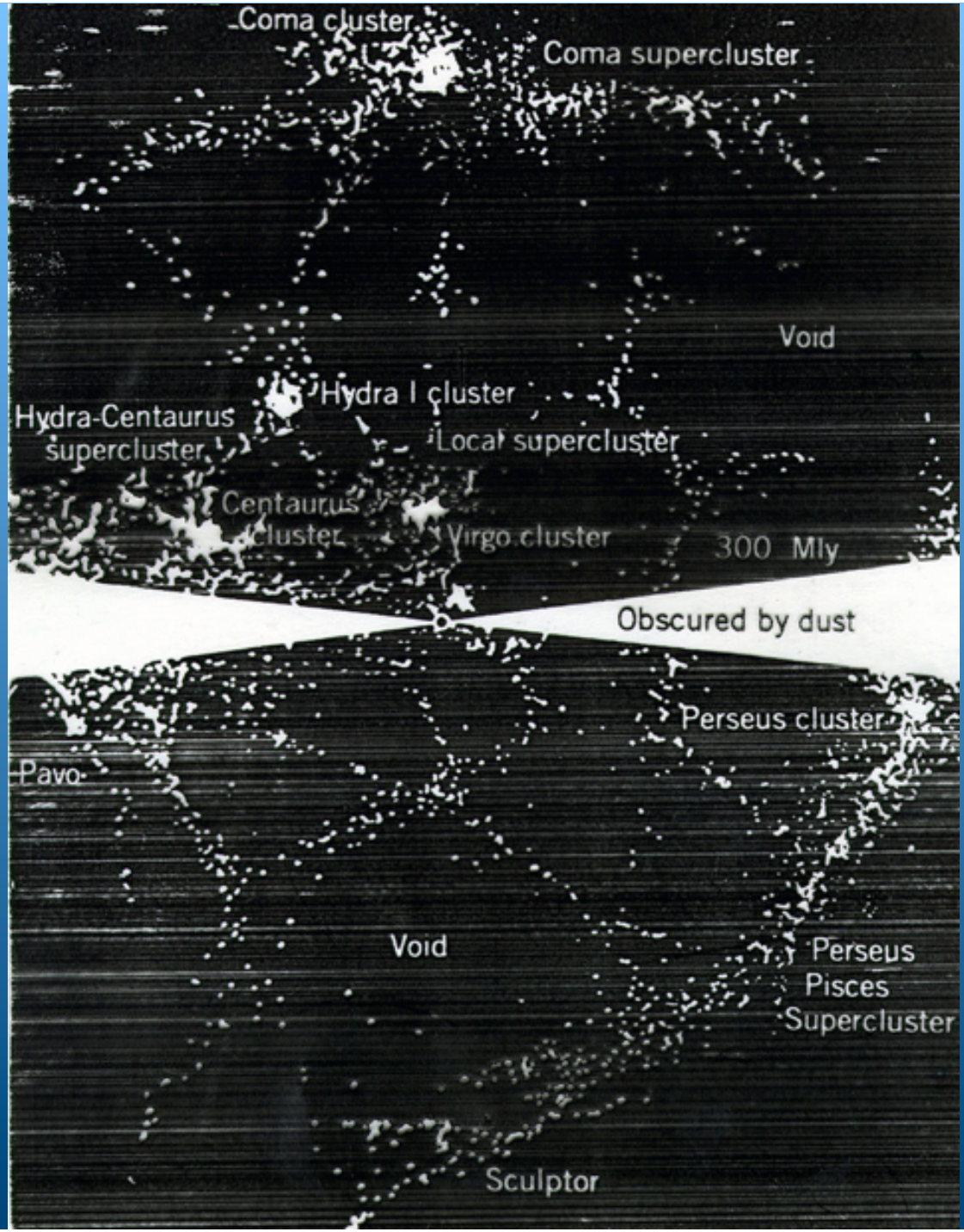
Coma cluster
Coma supercluster
Void
Hydra I cluster
Hydra-Centaurus supercluster
Local supercluster
Centaurus cluster
Virgo cluster
300 Mly
Obscured by dust
Perseus cluster
Pavo
Void
Perseus Pisces Supercluster
Sculptor

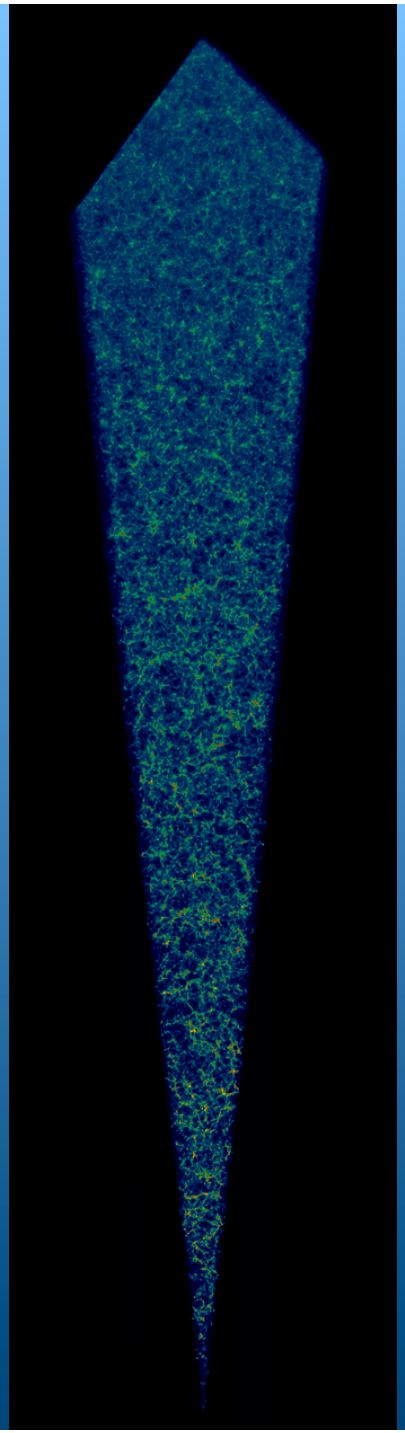

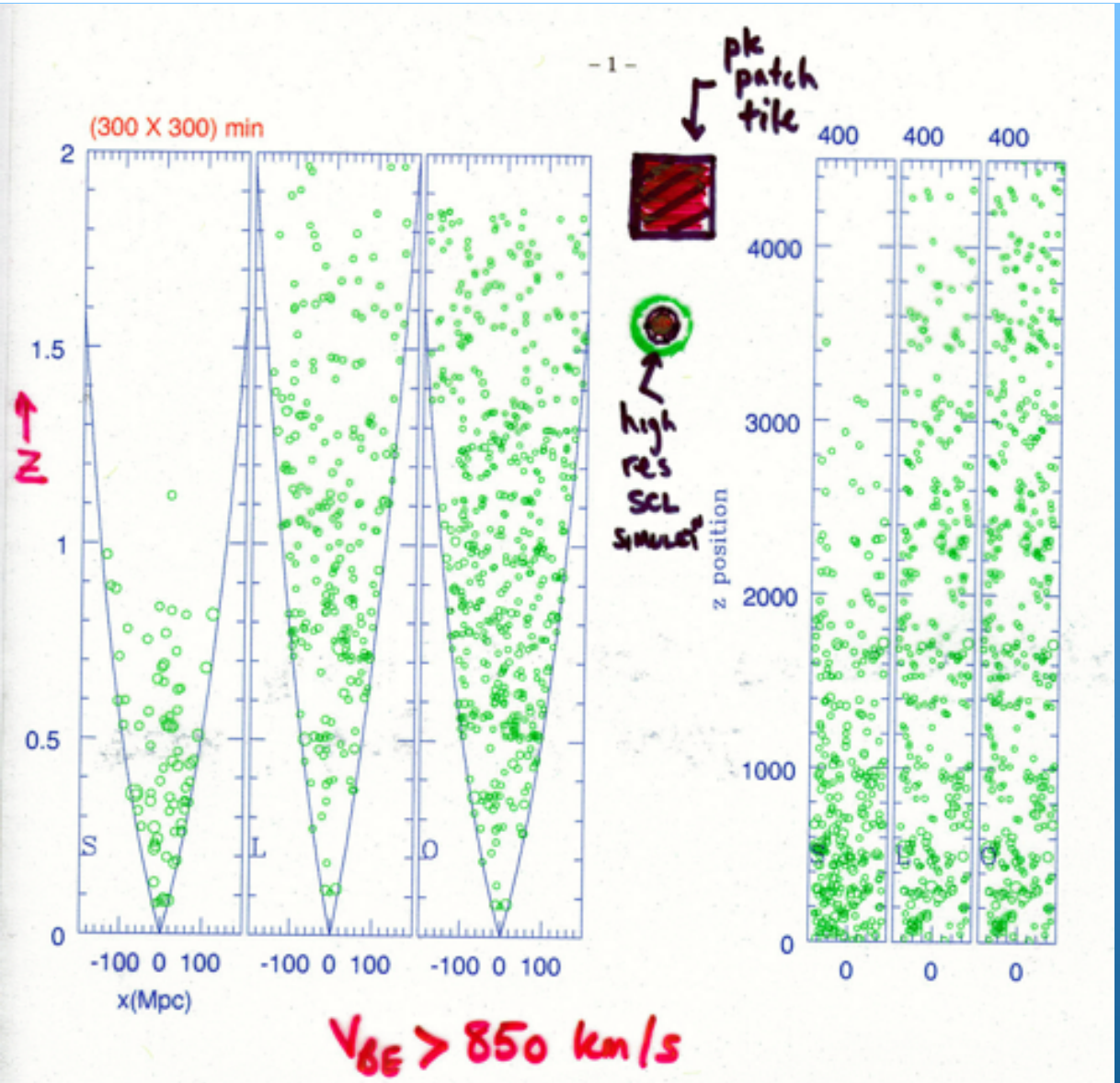

Fig. 1.— The redshift and comoving-space distributions of cluster peak-patches. Only the clusters with $v_{BE} > 850\,\mathrm{km\ s^{-1}}$ and baryonic mass above $10^{13}\,\mathrm{M}_\odot$. The 3 cosmologies shown, $\{S, \Lambda, O\}$CDM, all reveal large scale superclustering features, though more pronounced in OCDM and ΛCDM. Most dramatic of course is the dearth of impressive clusters at high redshift in the sCDM model.

300 Mpc Thick Slice

ΛCDM

z = 0 to 2

peak-patch clusters

interferometers c.f. Planck

ΔT/T
red < -30 x 10^{-6}
white <-2 x 10^{-6}
blue < -5 x 10^{-7}

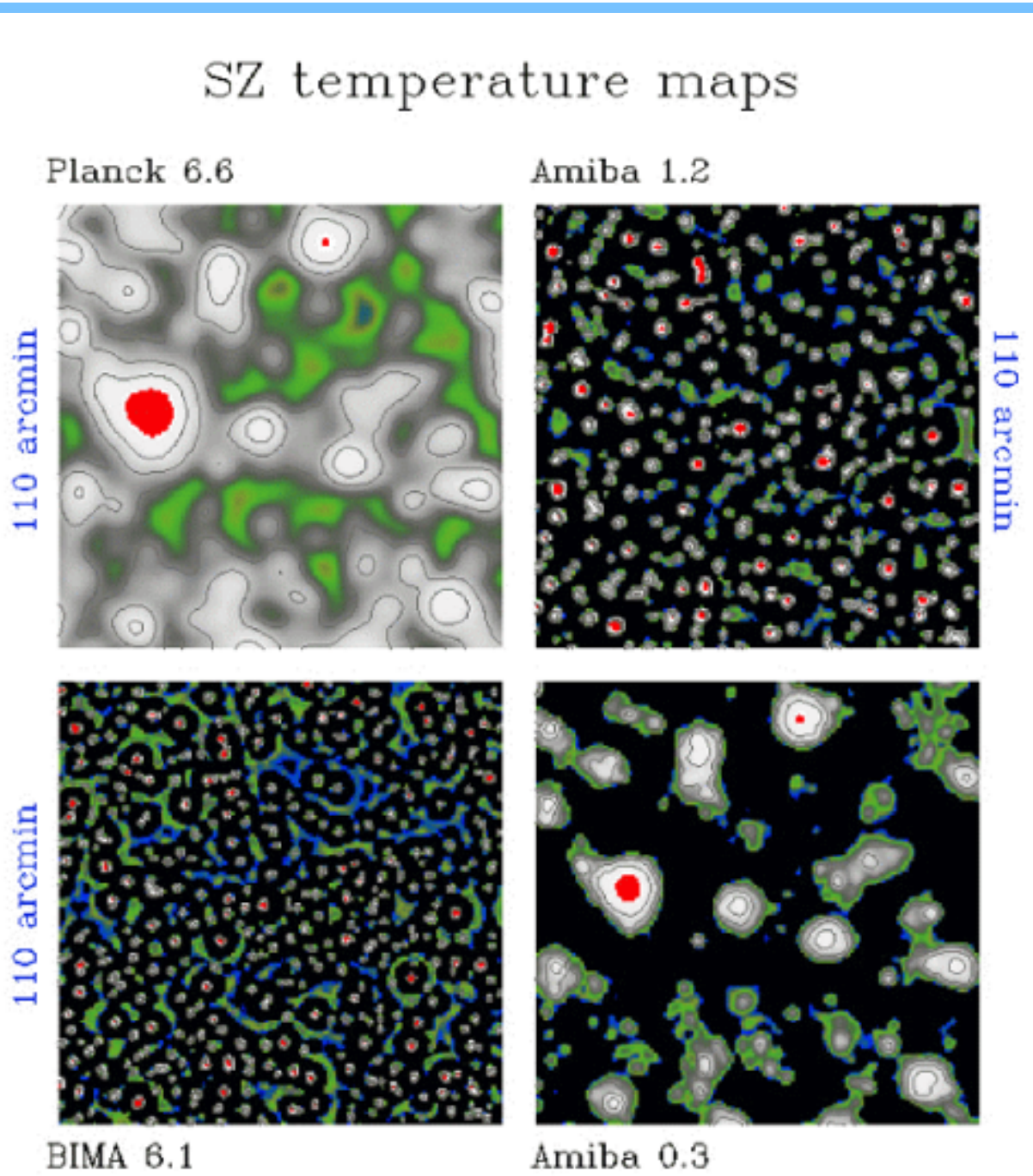

Cluster Peak Patches in Final State Space

(Eulerian)

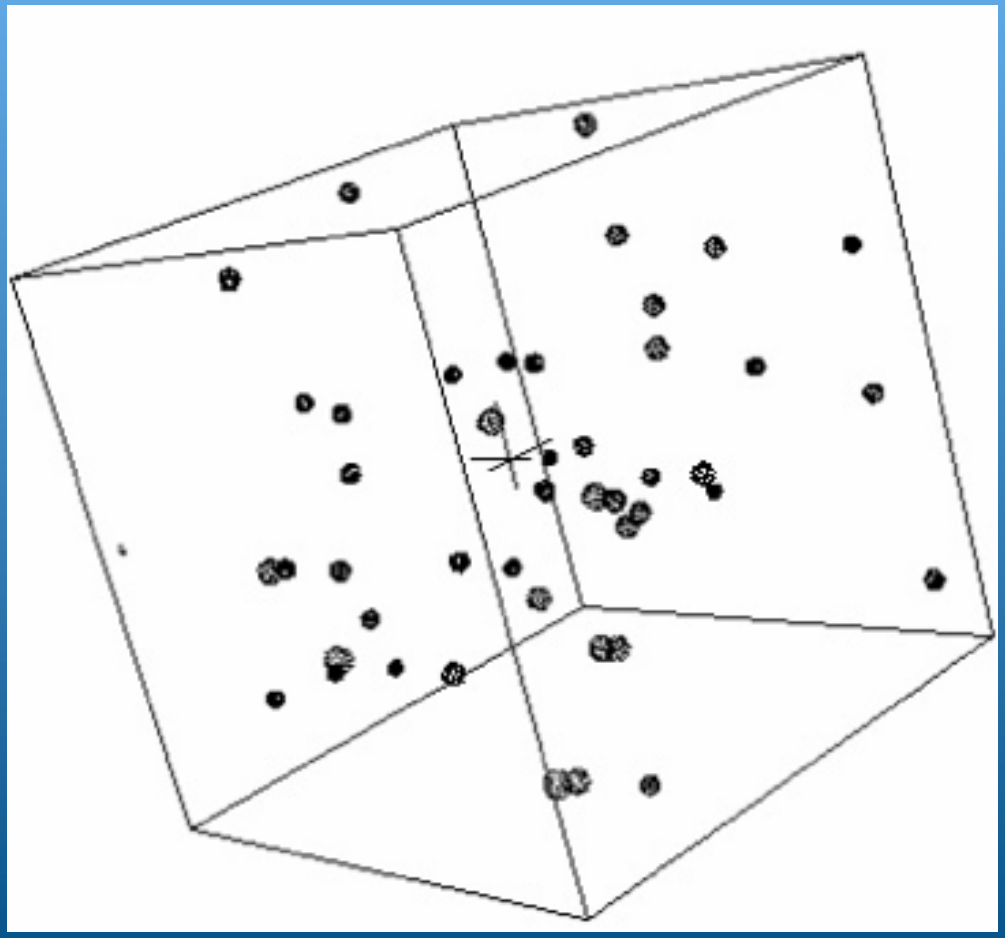

$(400\ \mathrm{Mpc})^3$ simulation

N-body groups in Final State Space

(Eulerian)

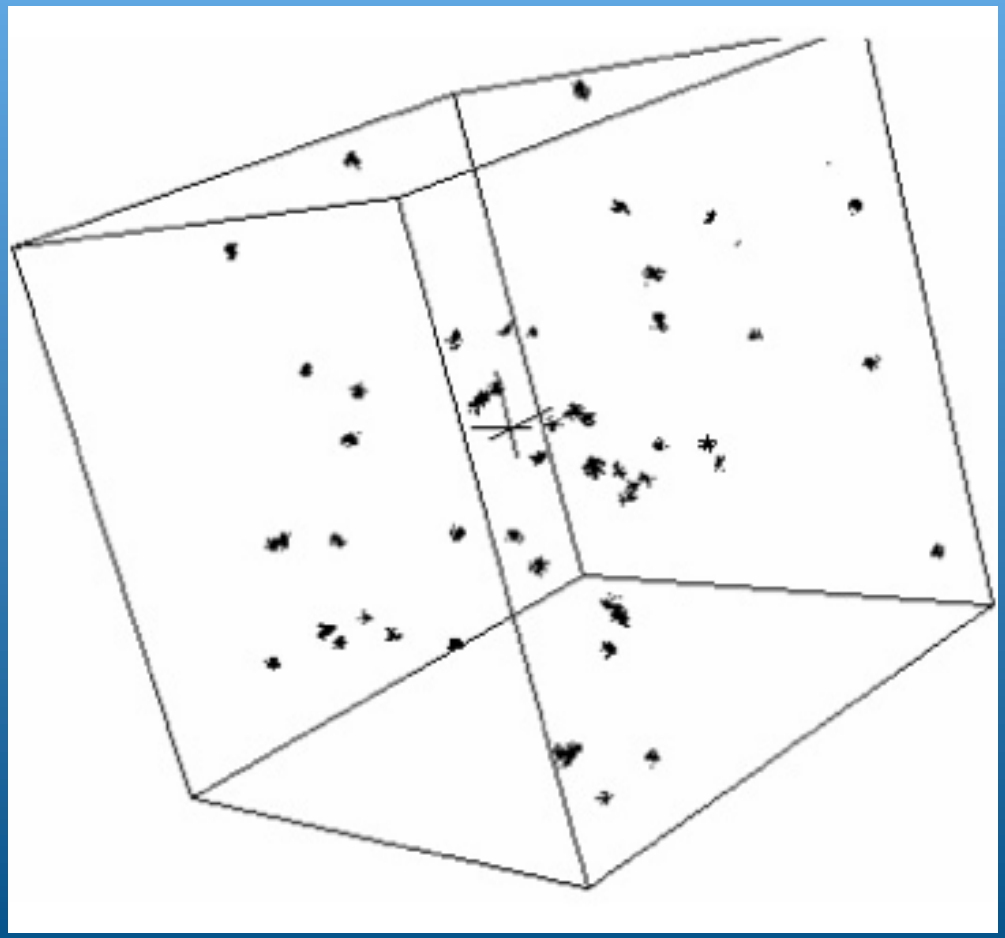

Cluster peak patches & N-body groups overlapped

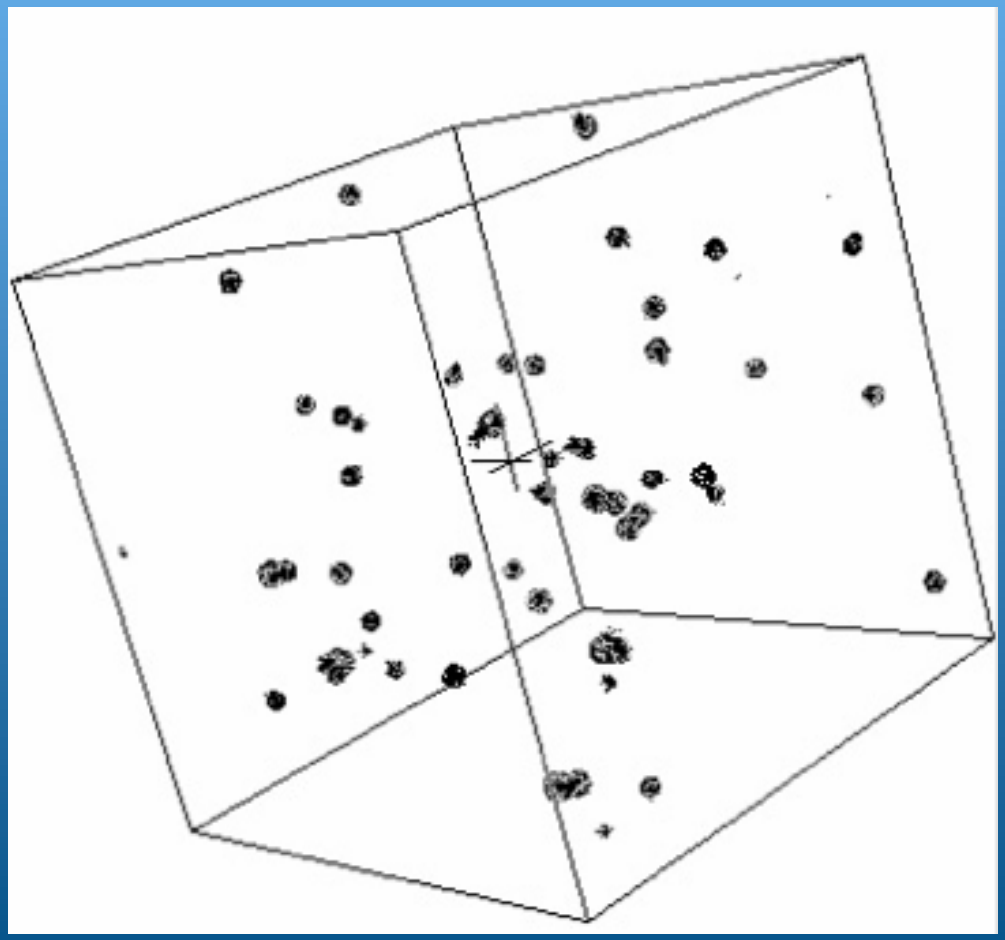

Molecular Picture of Filaments & Membranes in LSS

B + Kofman + Pogosyan 96-99

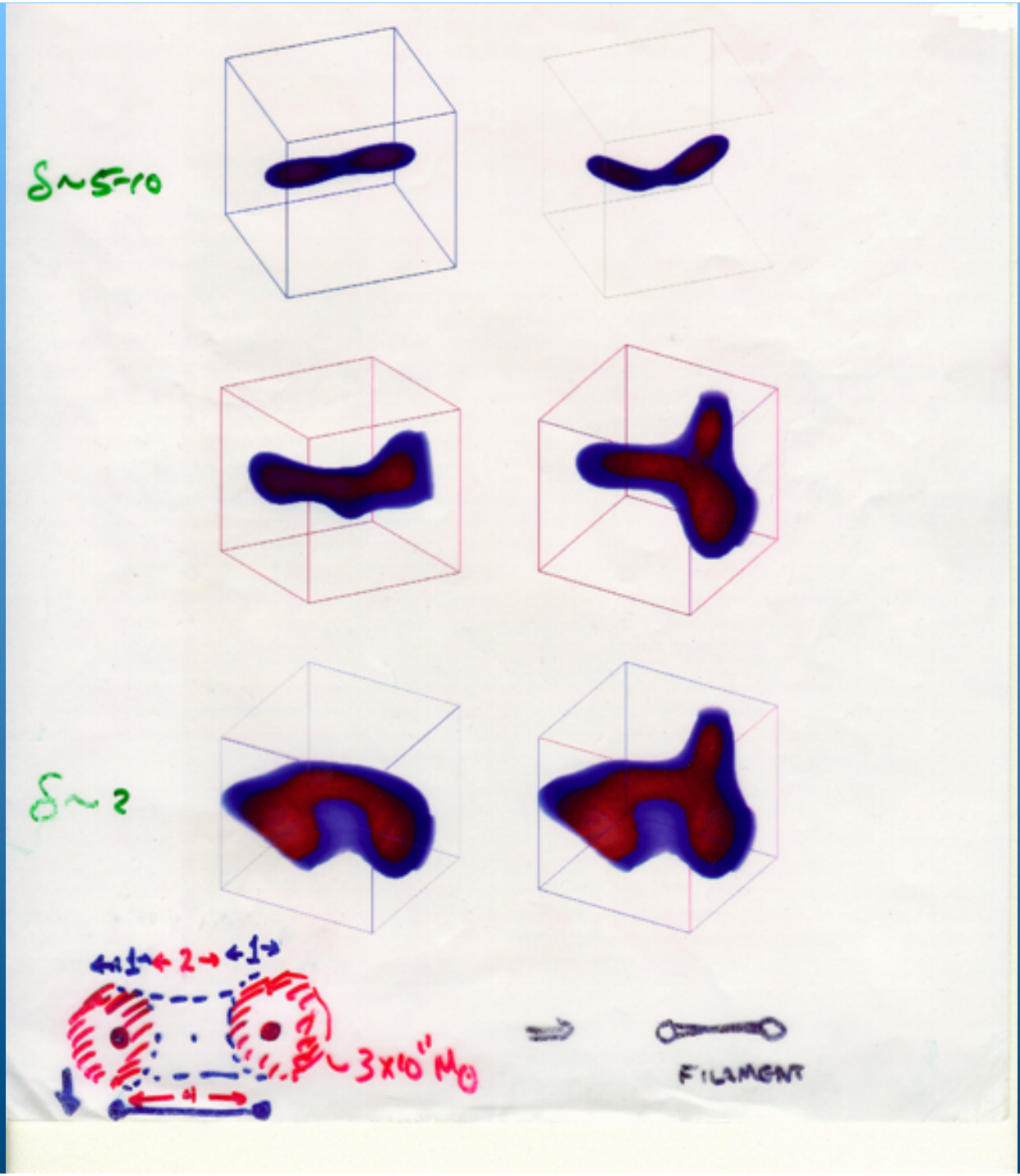

How the

Cosmic

Web

varies with

Density

Spectrum

tilt

$d\sigma_{\rho L}^2/d\ln k \sim k^{(n+3)}$

smoothing

$\sigma_{\rho L} = 0.65$

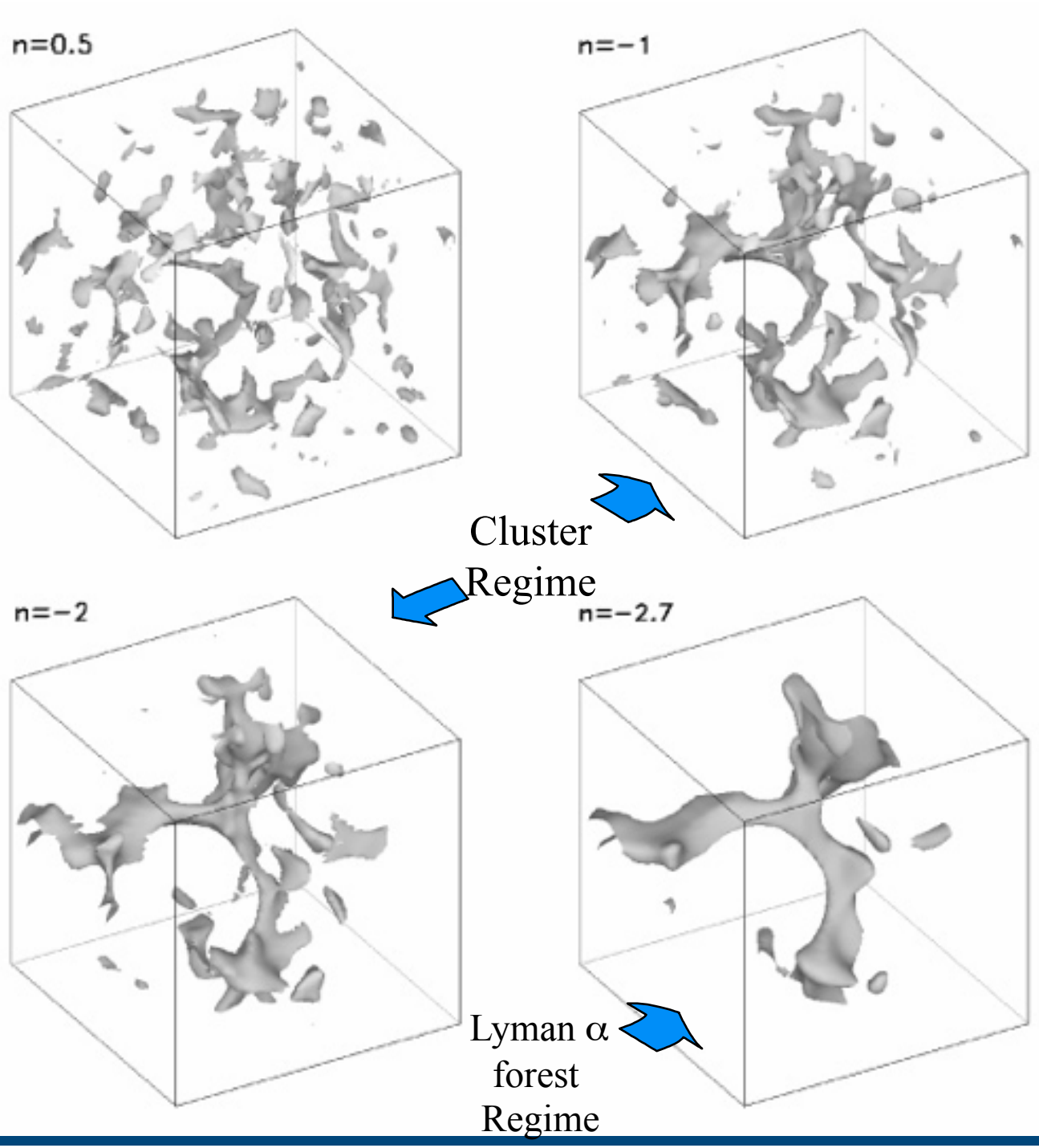

sample density field reconstruction from most massive peak-patch clusters

Smoothing
$\sigma_{\rho L} = 0.65$

Lagrangian (initial condition) space

Eulerian (final state) space

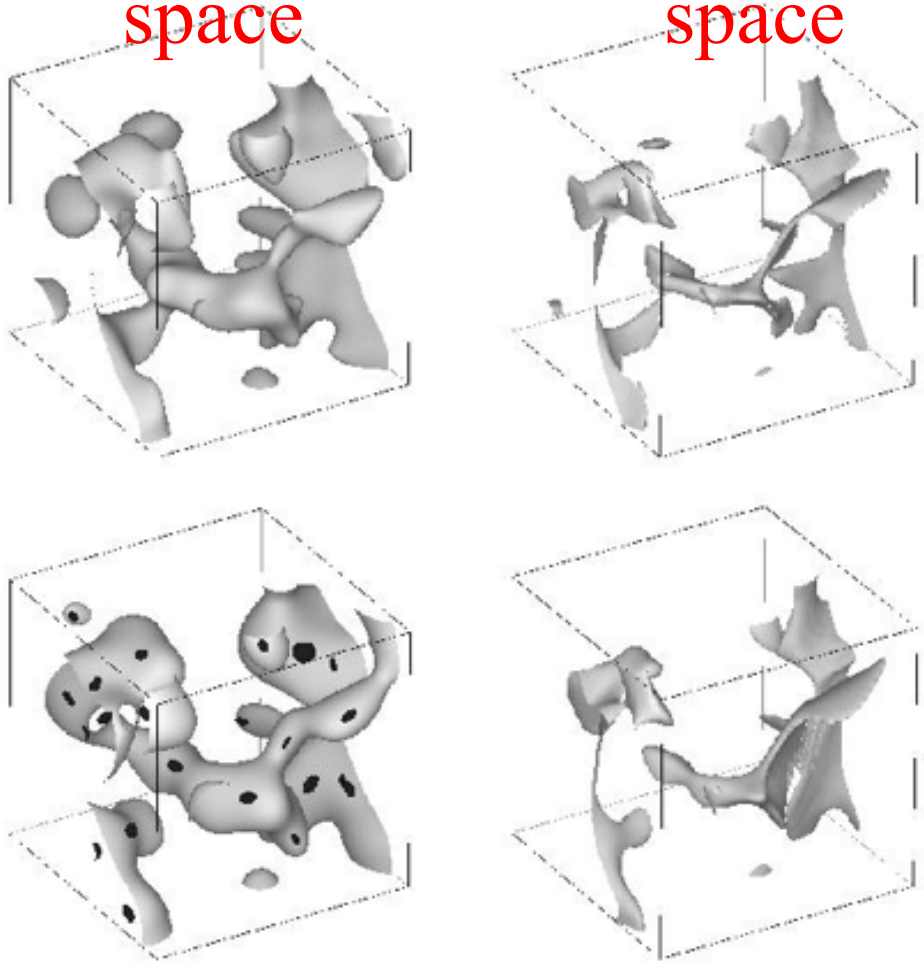

Contour level at percolation threshold

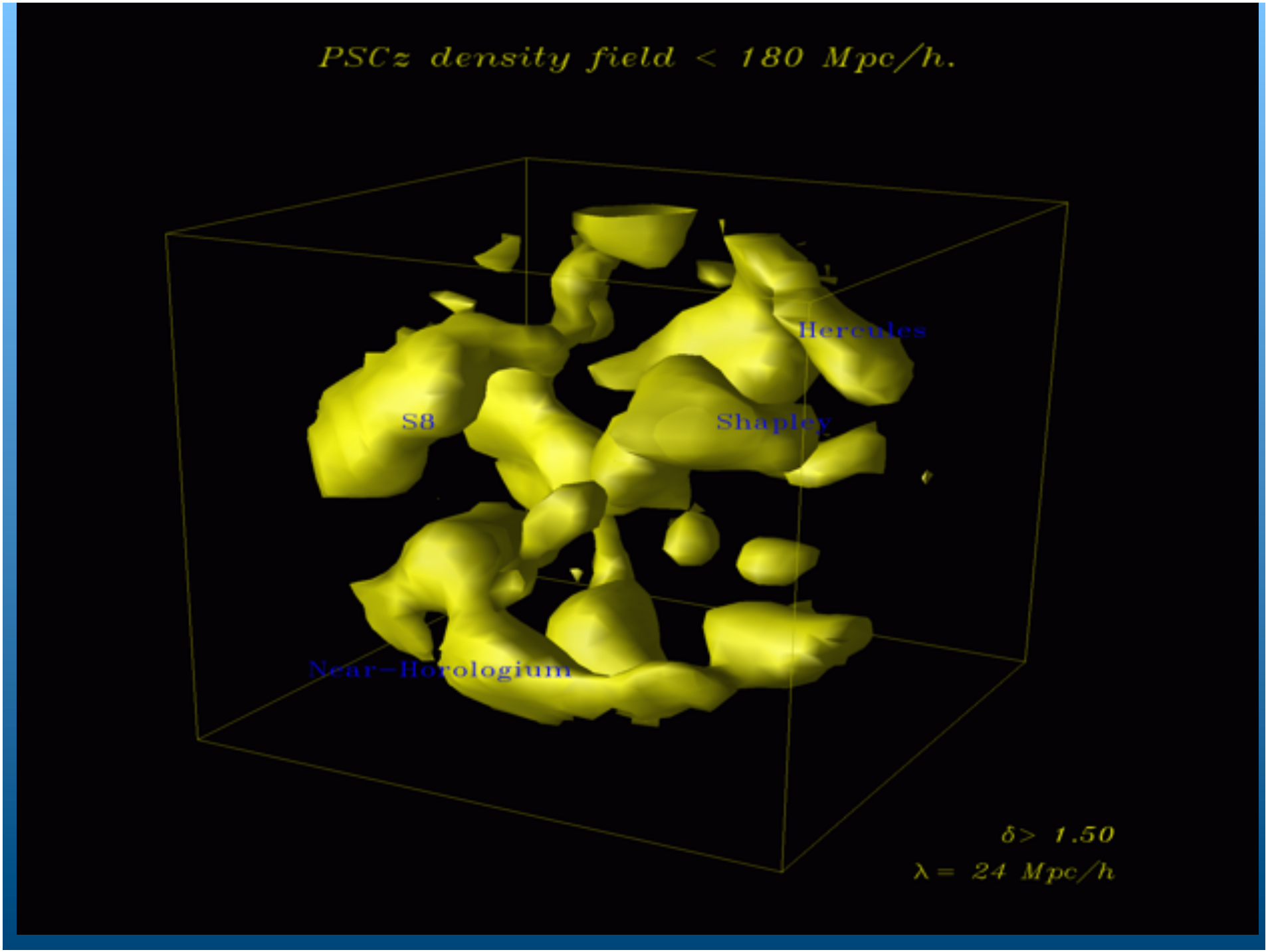
PSCz density field < 180 Mpc/h.
Hercules
S8
Shapley
Near−Horologium
δ> 1.50
λ = 24 Mpc/h

CorBor & Coma superclusters in the Century z-survey

(Geller etal 98)

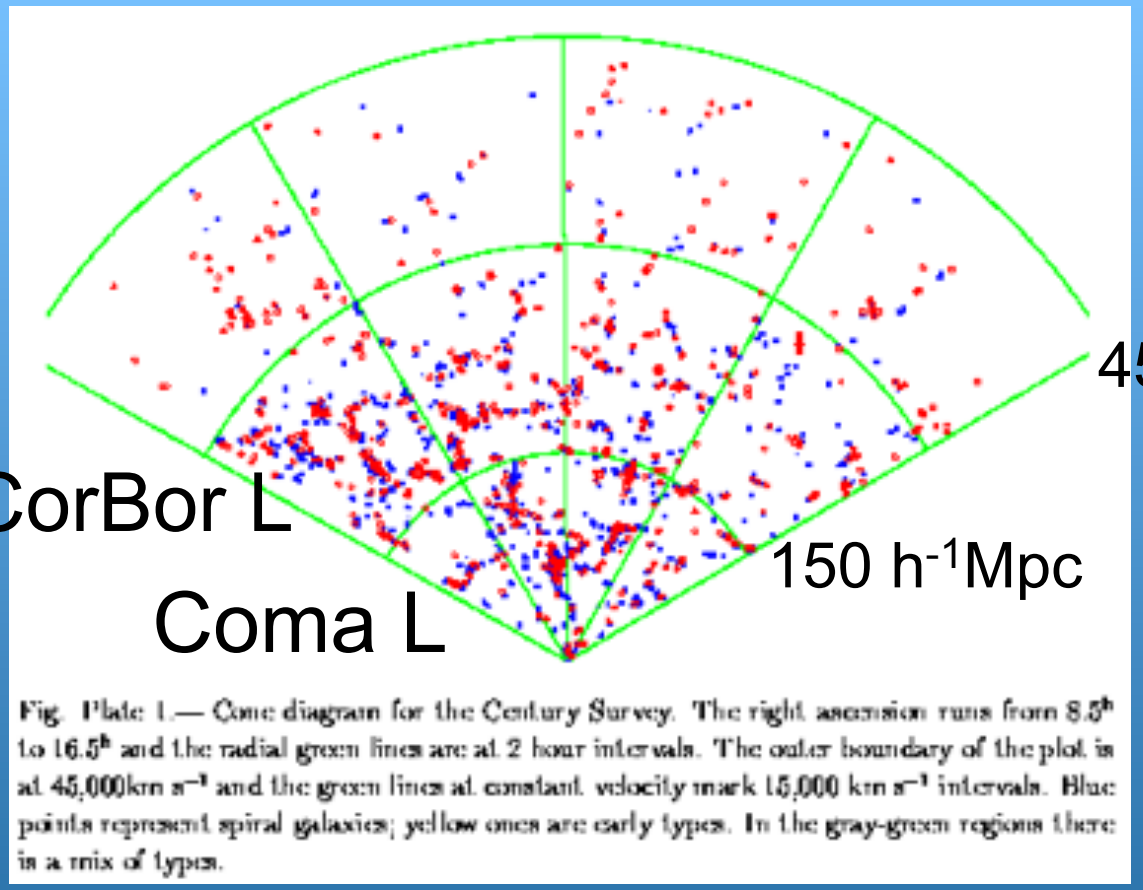

Fig. Plate 1.— Cone diagram for the Century Survey. The right ascension runs from 8.5^h to 16.5^h and the radial green lines are at 2 hour intervals. The outer boundary of the plot is at 45,000km s^{-1} and the green lines at constant velocity mark 15,000 km s^{-1} intervals. Blue points represent spiral galaxies; yellow ones are early types. In the gray-green regions there is a mix of types.

CorBor: biggest scl in Northern Sky 7 cls, M . 4 x 10^{16} $h^{-1}M_{\odot}$

$M/L_B(<20h^{-1}Mpc)$. 560 $h\,L_{\odot}/M_{\odot}$ Y S . 0.36 " 0.1 Small, Ma, Sargent, Hamilton 98

Hercules: 3 cls, .8x10^{16} $h^{-1}M_{\odot}$, 530 Y S . 0.34 " 0.1 Barmby,Huchra 98

Shapley: 20 cls, /10^{16} $h^{-1}M_{\odot}$, core+web Bordelli etal,, Drinkwater etal

c.f. CNOCI 14cls Y S . 0.19 " 0.06 " 0.04 Carlberg etal 96,97

X-ray cls $\sigma = (.3".1) h^{-1/2}$

SZ cls (45) (.25 ".04) h^{-1} Mohr etal

scl lensing (3 cls) z=.4 σ-0.3 or so Kaiser & Luppino

cl baryon fraction + BBN σ-0.3 " .05

cl abundance evolution σ-0.25 " .1 e.g. Bahcall etal 99

CorBor: biggest scl in Northern Sky 7 cls, M . 4 x 10^{16} $h^{-1} M_{\odot}$

$M/L_B(<20h^{-1}\mathrm{Mpc})$. 560 $h\, L_{\odot}/M_{\odot}$ Y σ . 0.36 " 0.1 Small, Ma, Sargent, Hamilton 98

Hercules: 3 cls, .8x10^{16} $h^{-1} M_{\odot}$, 530 Y σ . 0.34 " 0.1 Barmby,Huchra 98

Shapley: 20 cls, /10^{16} $h^{-1} M_{\odot}$, core+web Bordelli etal,, Drinkwater etal

c.f. CNOCI 14cls Y σ . 0.19 " 0.06 " 0.04 Carlberg etal 96,97

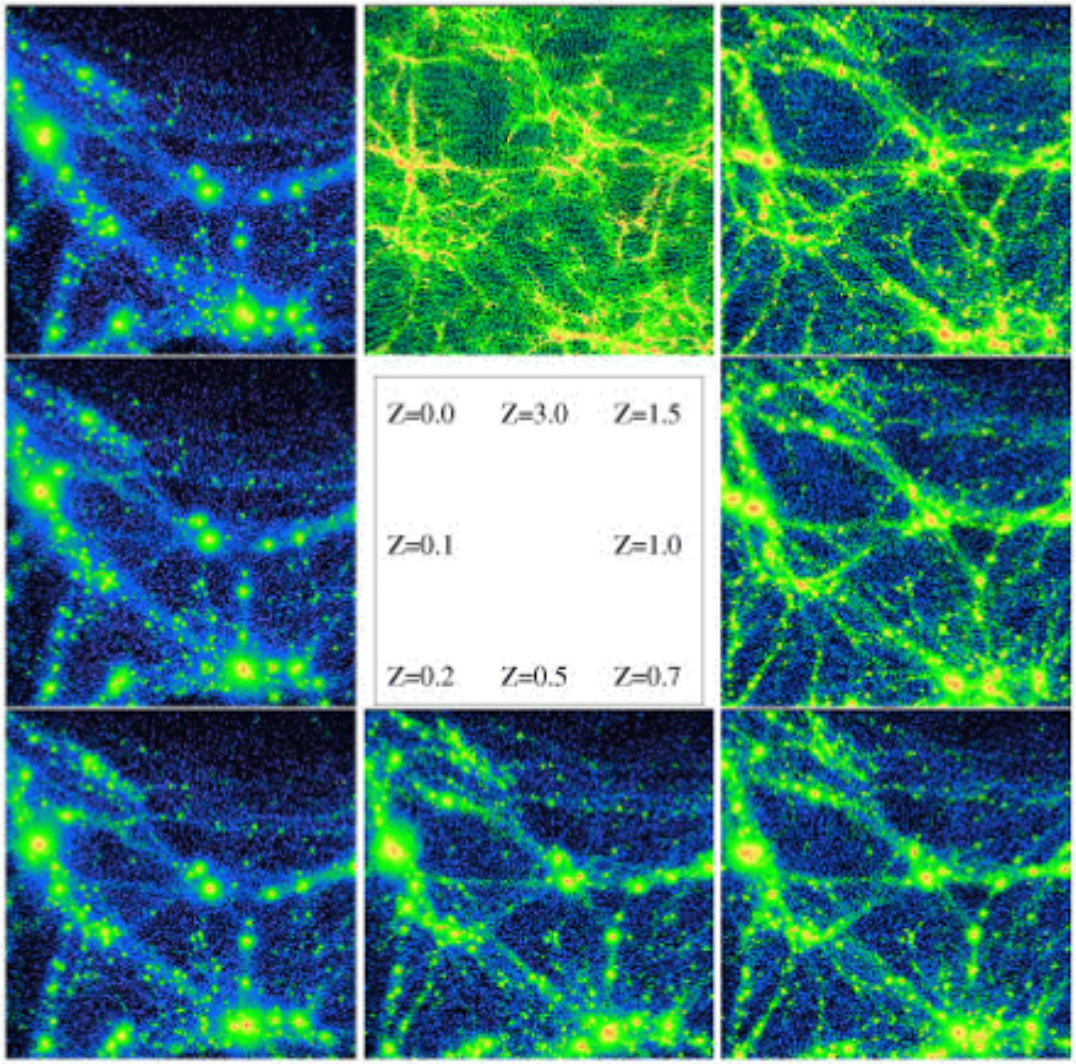

Gas density in a $\sim$ 100 Mpc (comoving diameter) patch at redshifts z=3, 1.5, 1, 0.7, 0.5, 0.2, 0.1 and 0.0 (clockwise from the top) from a 1.6 million particle constrained-field "super-cluster" simulation, with HR region 104 Mpc, MR region 166 Mpc and LR region 266 Mpc, with wave coverage to $k^{-1} = 1000$ Mpc, the very long waves entering through a self consistent mean tidal field. 17 peak patches (found at $z = 0$) were used as constraints, defining a complex supercluster region in a 400 Mpc simulation. The cosmology shown is ΛCDM (σ_8=0.91, h=0.7, $\Omega_{o,r}$=0.3349).

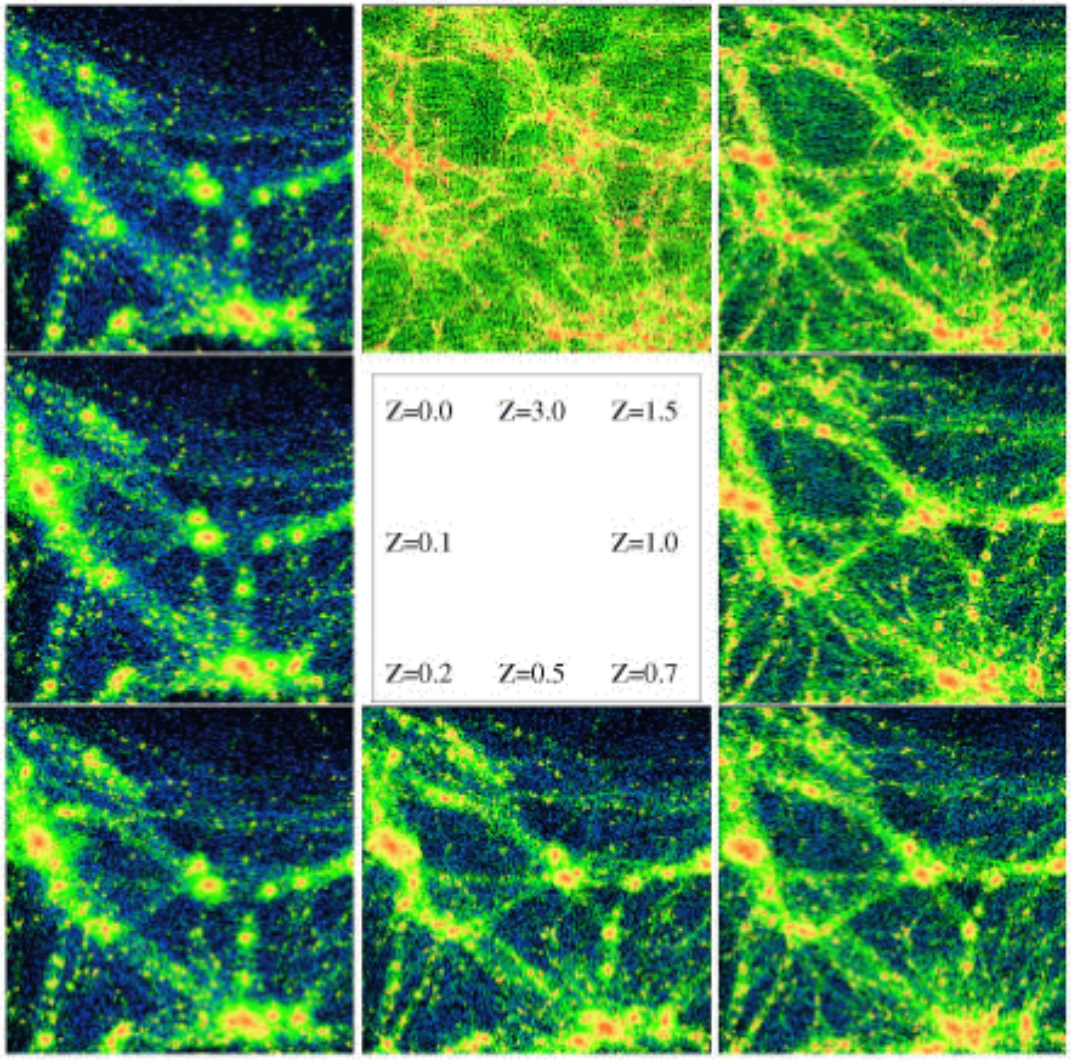

Dark matter density in a ~ 100 Mpc (comoving diameter) patch at redshifts z=3, 1.5, 1, 0.7, 0.5, 0.2, 0.1 and 0.0 (clockwise from the top) from a 1.6 million particle constrained-field "super-cluster" simulation, with HR region 104 Mpc, MR region 166 Mpc and LR region 266 Mpc, with wave coverage to $k^{-1} = 1000$ Mpc, the very long waves entering through a self consistent mean tidal field. 17 peak patches (found at $z = 0$) were used as constraints, defining a complex supercluster region in a 400 Mpc simulation. The cosmology shown is ΛCDM (σ_8=0.91, h=0.7, Ω_{nr}=0.3349).

Constrained Supercluster Simulation Comparing 3 Cosmologies

Blank field SZ >Counts' from clusters stronger test

$\Delta T/T$

red < -30×10^{-6}

white <-2×10^{-6}

blue < -5×10^{-7}

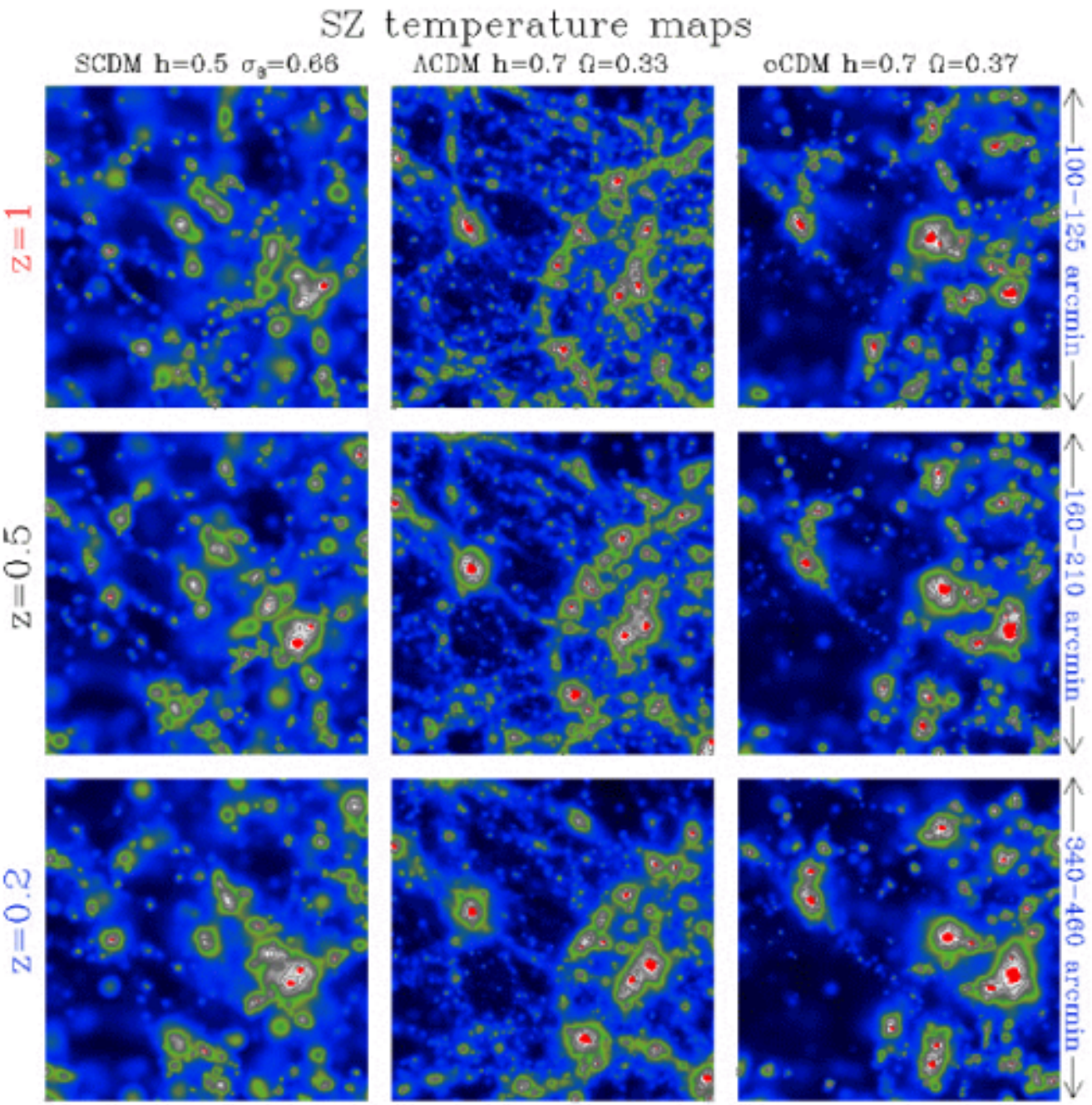

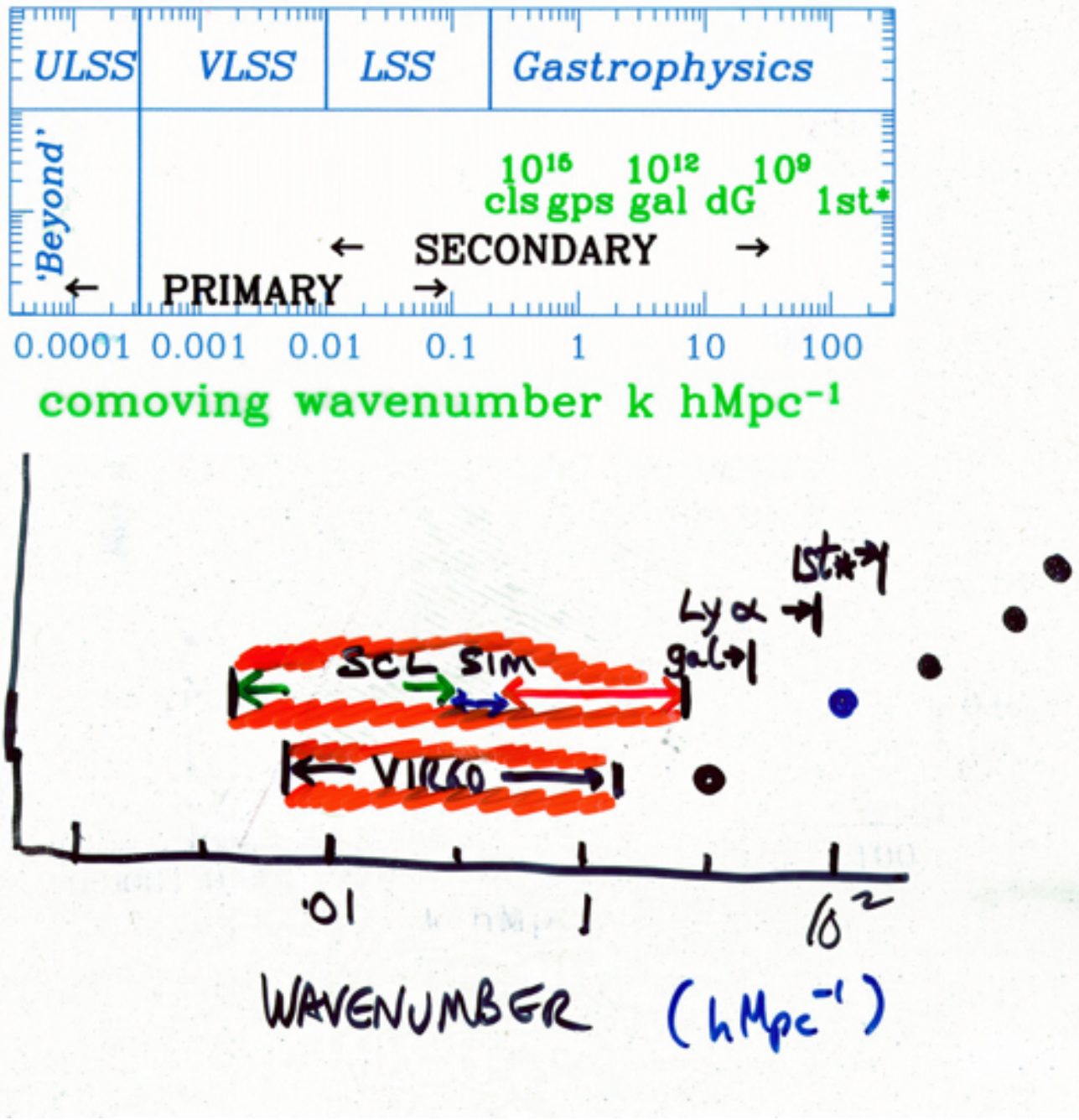
ULSS
VLSS
LSS
Gastrophysics
'Beyond'
10^{16} 10^{12} 10^{9}
cls gps gal dG 1st*
← SECONDARY →
← PRIMARY →
0.0001 0.001 0.01 0.1 1 10 100
comoving wavenumber k hMpc^{-1}
1st*
Ly α
gal
SCL SIM
VIRGO
·01
1
10^{2}
WAVENUMBER (hMpc^{-1})

ΛCDM

z = 0 to 2

peak-patch clusters

interferometers c.f. Planck

ΔT/T

red < -30 x 10^{-6}

white <-2 x 10^{-6}

blue < -5 x 10^{-7}

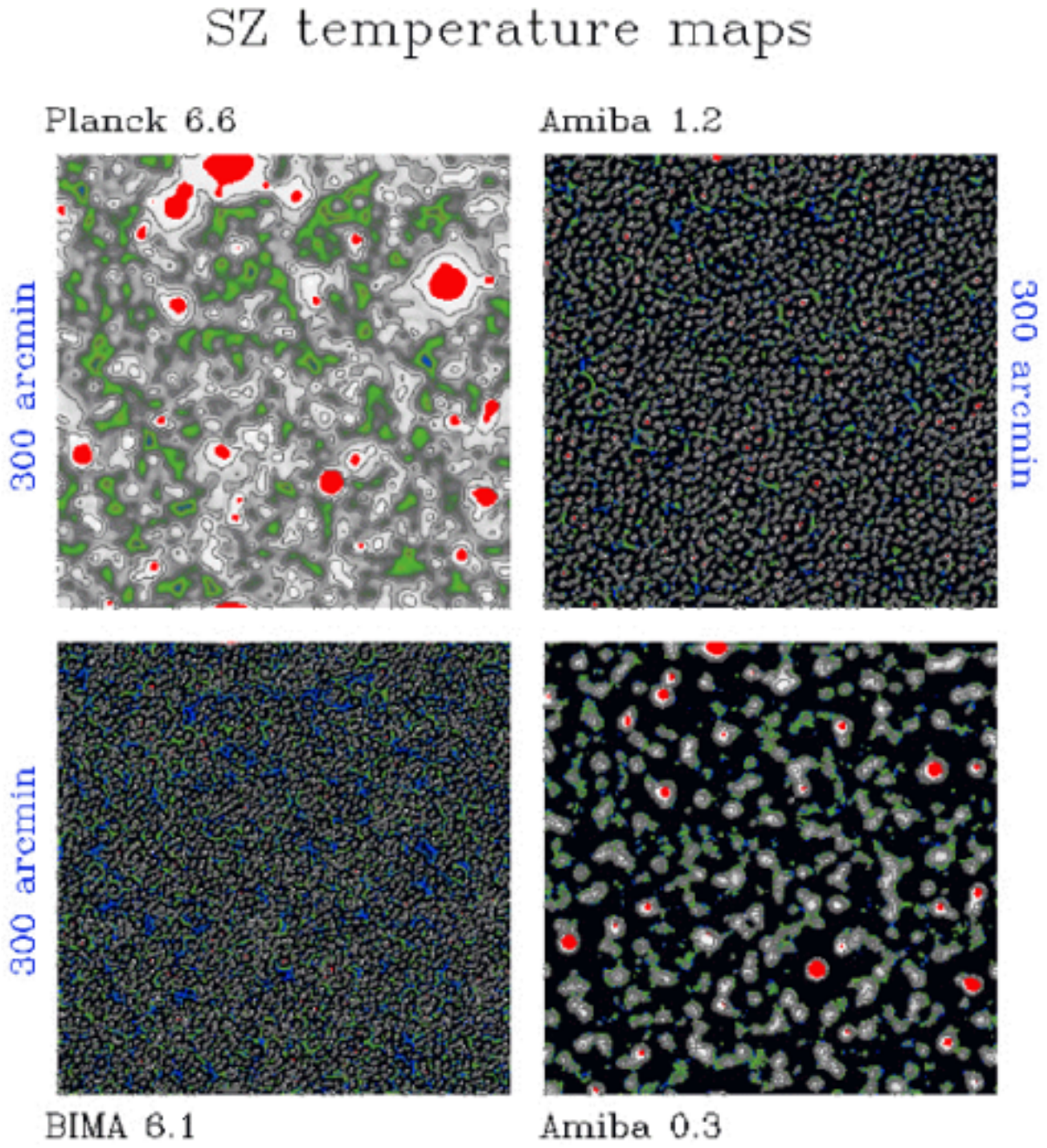

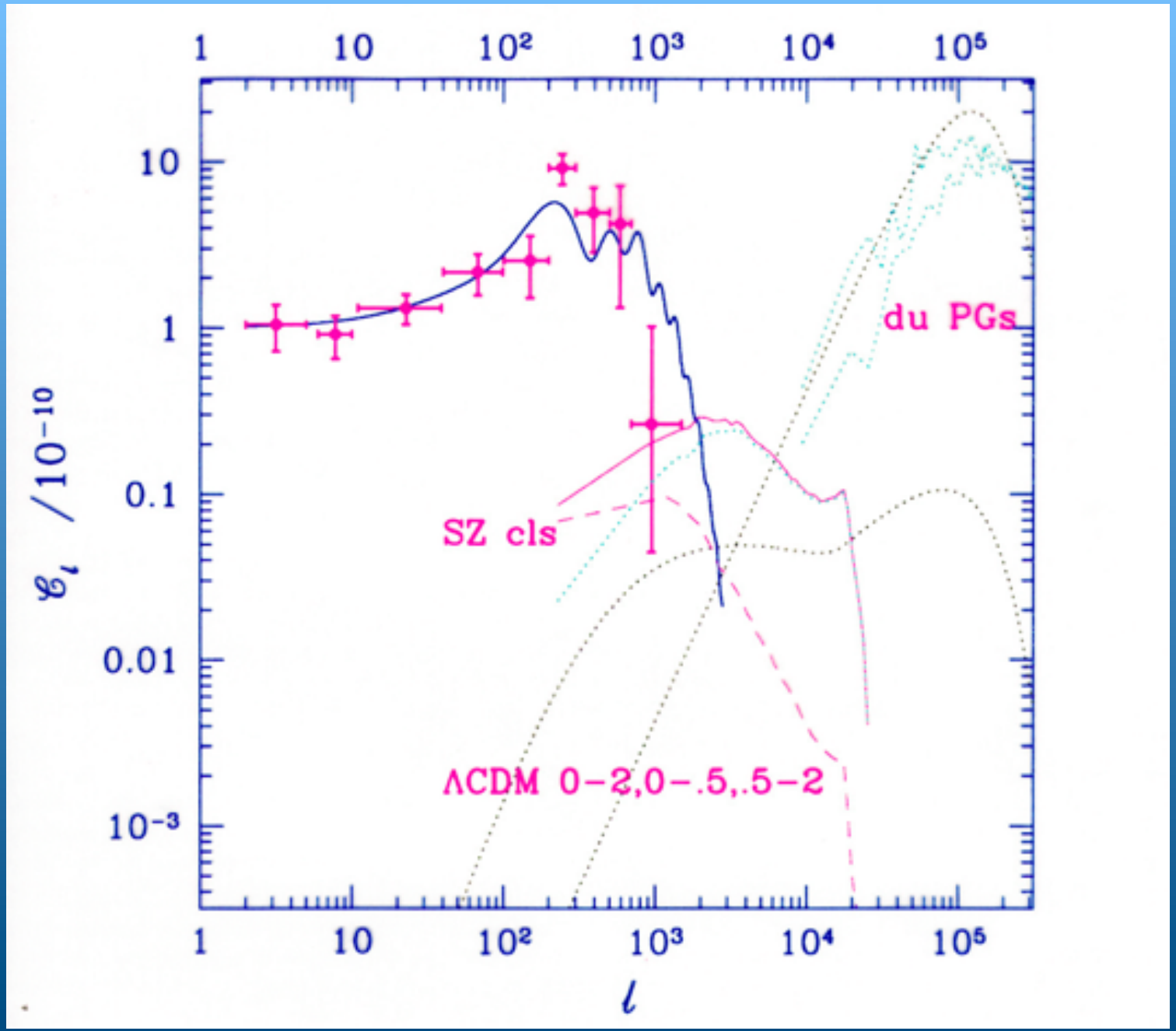
1
10
10²
10³
10⁴
10⁵
10
1
0.1
0.01
10⁻³
$\mathscr{C}_\ell$ /10⁻¹⁰
du PGs
SZ cls
ΛCDM 0-2,0-.5,.5-2
ℓ

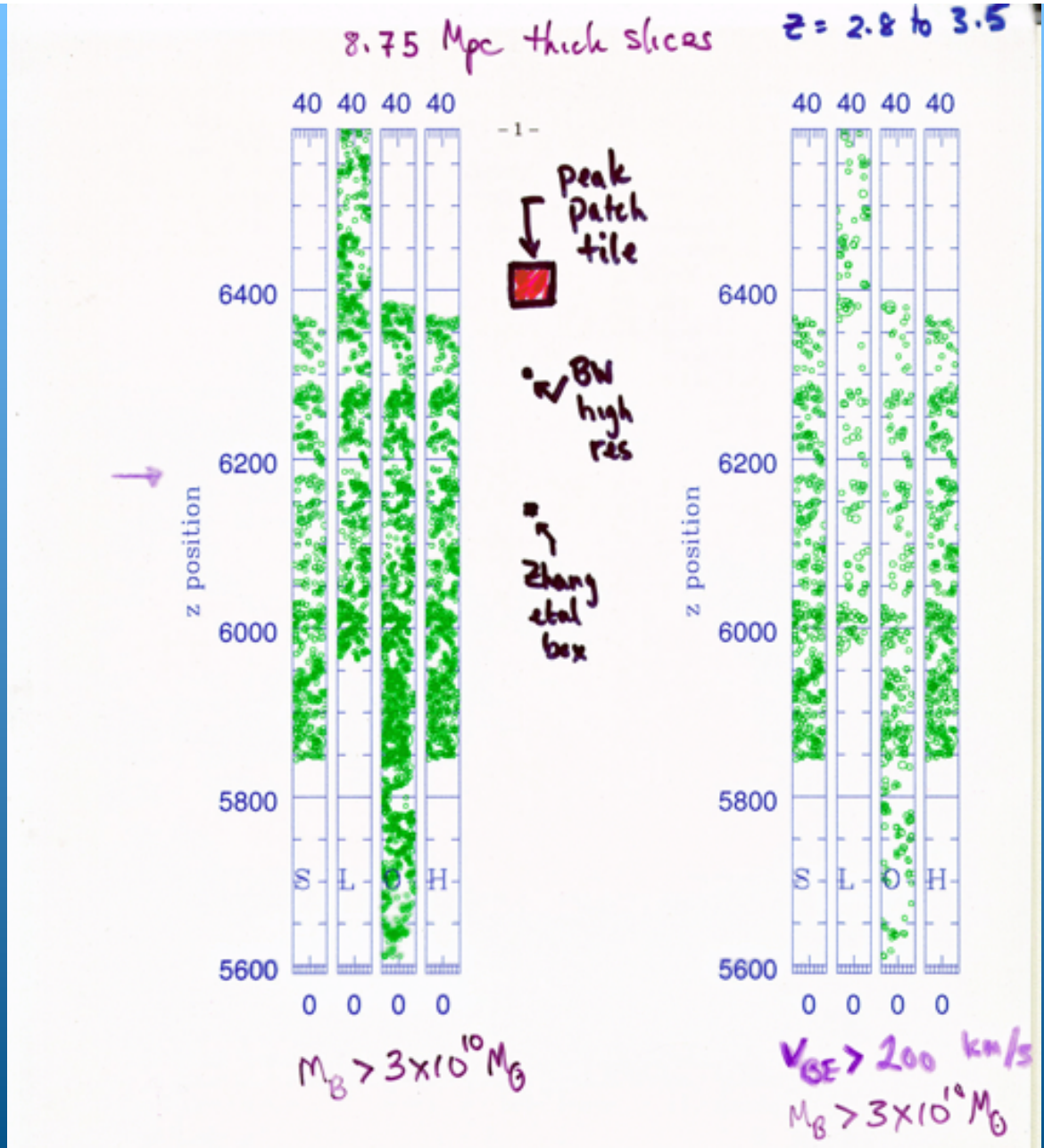

Fig. 1.— The comoving-space distributions of galactic halo peak-patches. Left has baryonic mass above $3 \times 10^{10}\,M_\odot$, right has a $v_{BE} > 200\,\mathrm{km\ s^{-1}}$ cut as well. The slice is 8.75 Mpc think, and the tiling boxes were 40 Mpc. The 4 cosmologies shown, $\{S, \Lambda, O, H\}$CDM, all reveal large scale features, though more pronounced in OCDM and ΛCDM.

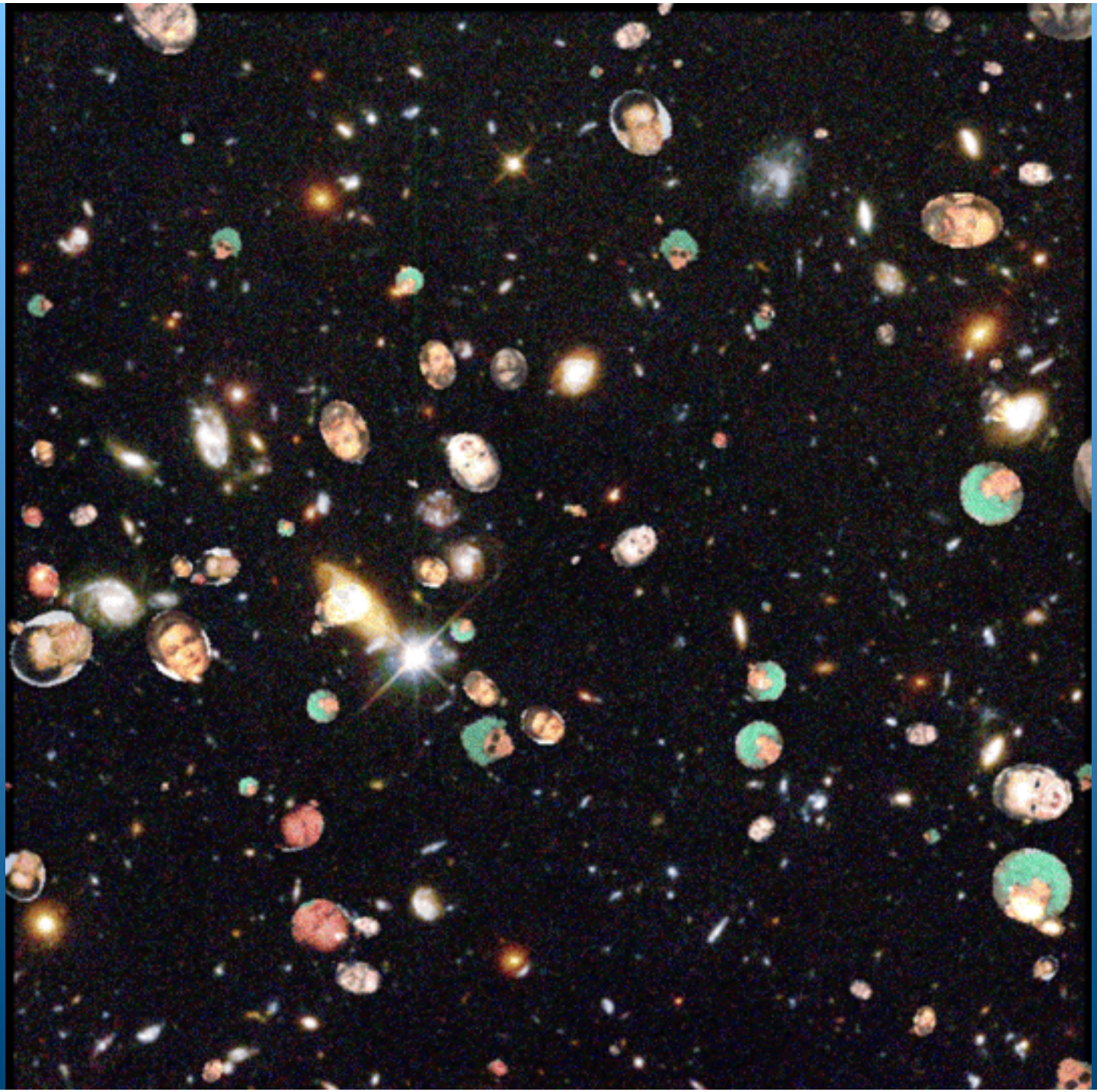

Hubble Deep Field

\+

some redshifts

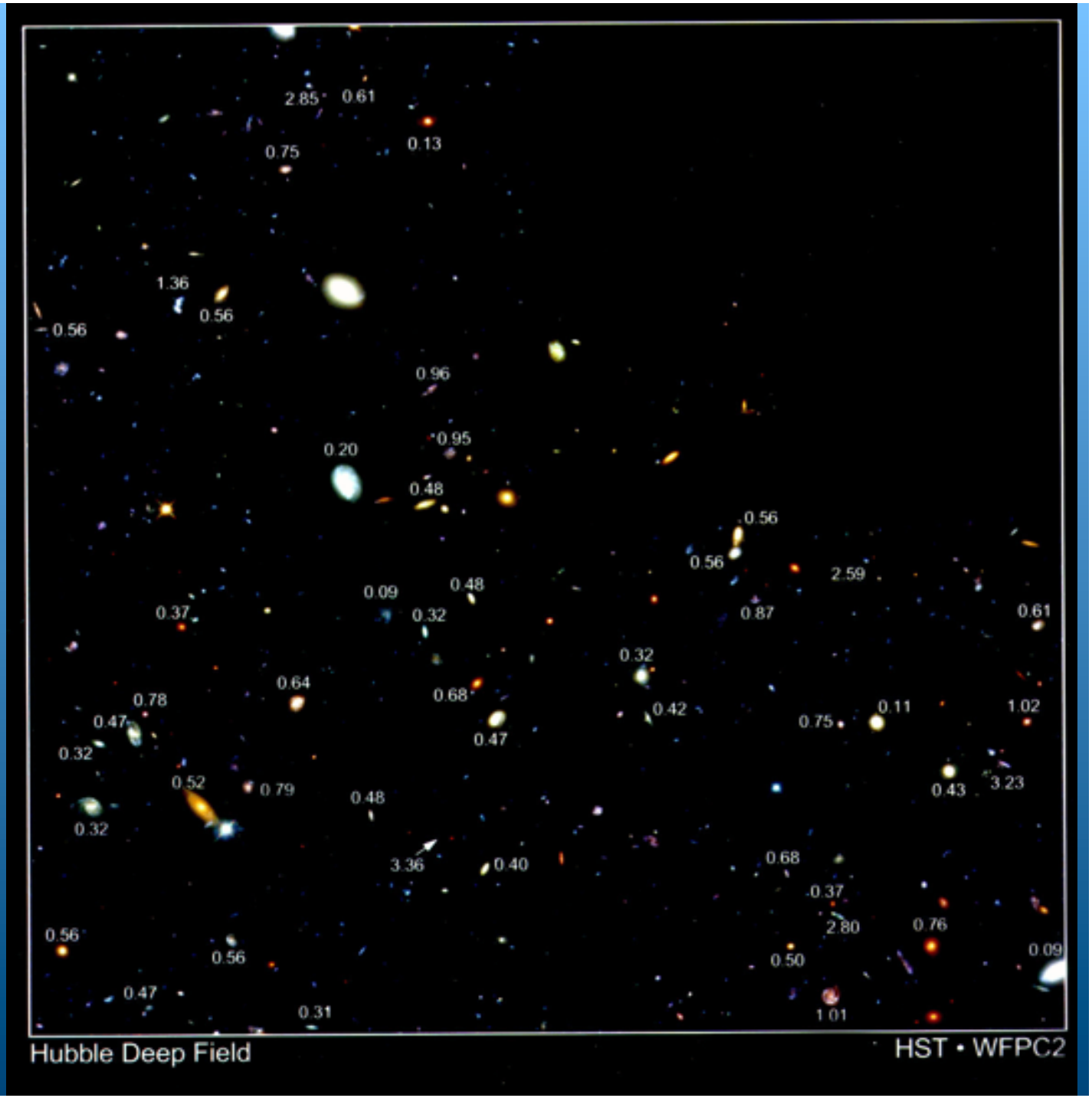

… but the optical is literally only half the story!

In the local Universe, about 40% of stellar luminosity emerges as thermally re-radiated emission by cool dust.

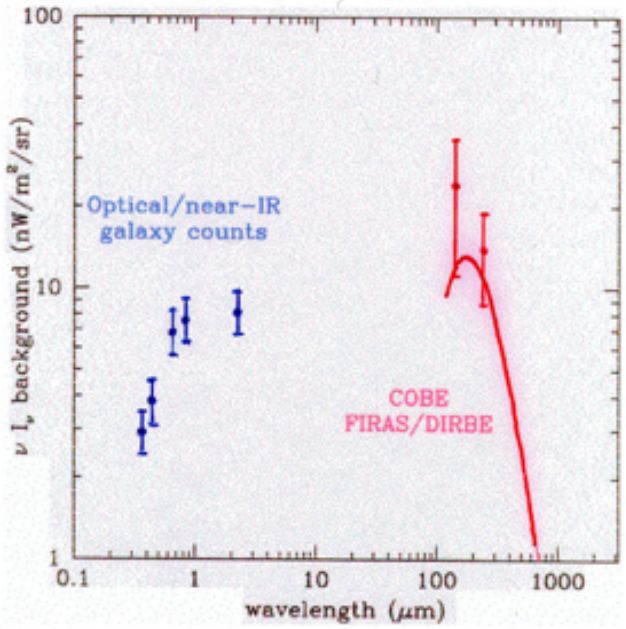

Rough equivalence of energy content in integrated optical and far-IR/sub-mm extragalactic backgrounds suggests that this dust continues to be important at high redshifts

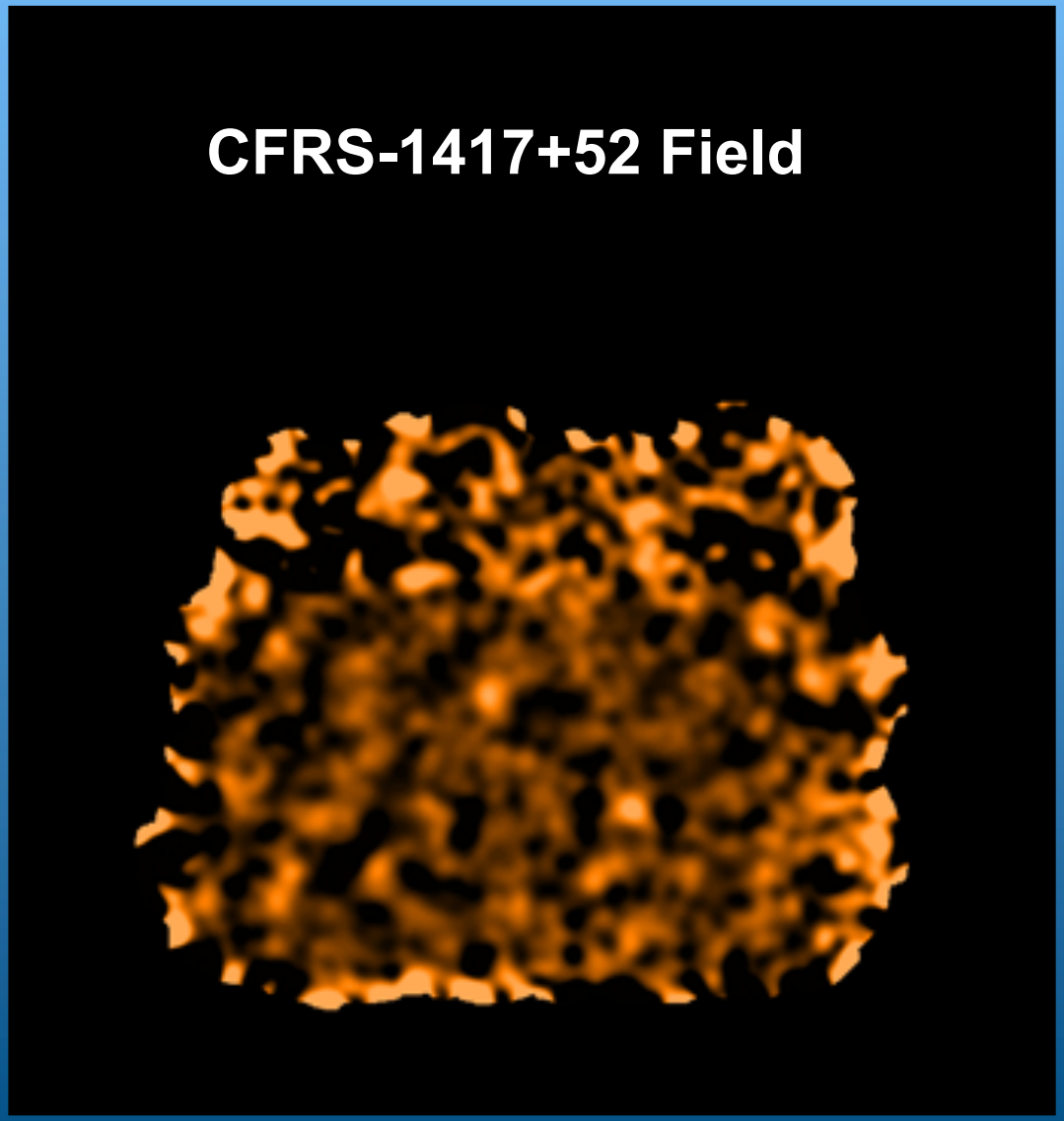

Canada-UK Deep Sub- mm Survey (CUDSS)

Simon Lilly (Toronto)
Steve Eales (Cardiff)
Walter Gear (UCLondon)
Dick Bond (Toronto)
Tracy Webb (Toronto)
Loretta Dunne (Cardiff)
+ many others

Goal:

cover two
8 x 8 arcmin^2 regions
to a 1σ 1 mJy level with SCUBA
on JCMT
complemented by deep ISO/WIRE
mid-IR, VLA radio and CFHT/HST
optical & near-IR images

for studies of galaxy formation and evolution and CMB foreground anisotropies

JCMT observations to be
completed January 2000
(60 x 8-hr shifts)

{ Eales Lilly Gear B

A Canada-UK Deep Survey with SCUBA*

***Sub-mm Common User Bolometer Array**
(Walter Gear, ROE)

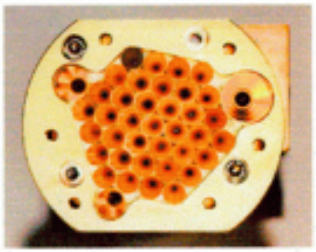

← 850 μm
450 μm →

SCUBA Sensitivity:

3σ ~ 2.7-3.0 mJy at 850 μm in 8-10 hours ⇒ detect 10^{12} L_O to z ~ 6.

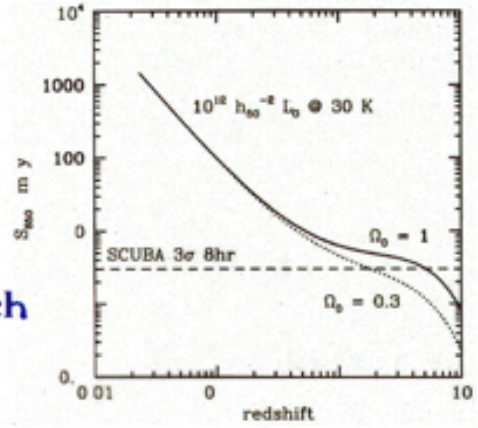

N.B. objects do not get much fainter beyond z = 0.5! →

Survey Goal: to identify the sub-mm background, to search for high luminosity highly obscured objects (proto-ellipticals?)

SCUBA data

(January and March 1998)

8-10 hr integrations in CFRS-03, CFRS-10 fields plus mosaic in the CFRS-14 field

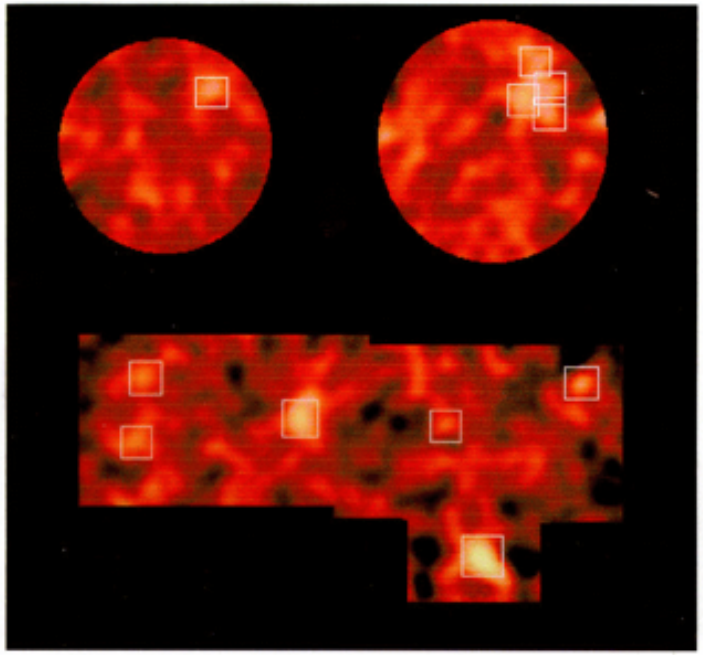

11 sources detected at 850 μm in 20 arcmin^2 with $S_{850} > 3$ mJy

⇒ 25% of the Puget/Fixsen COBE/FIRAS background

Cluster Survey of Lens-Amplified submm sources

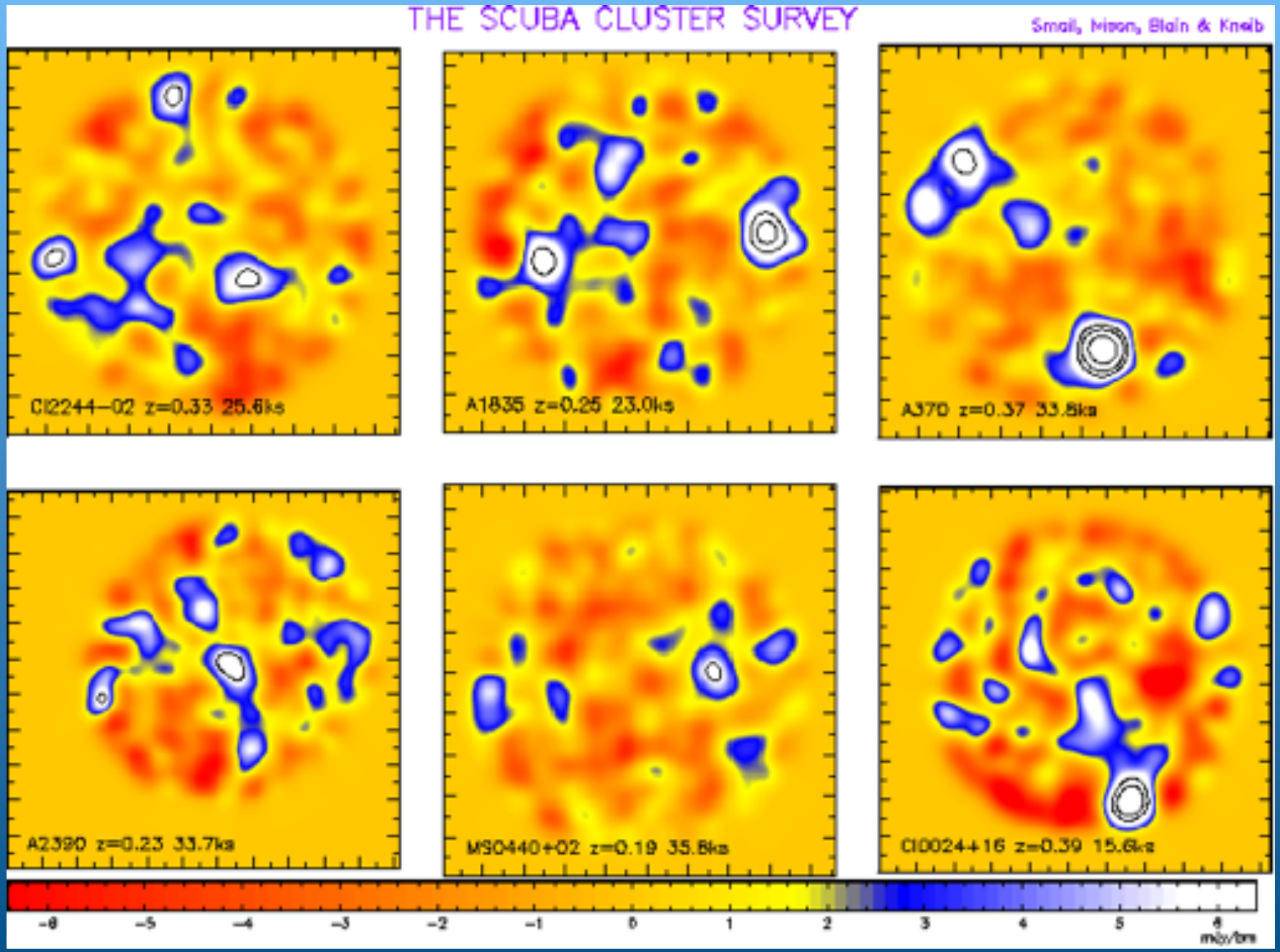

Smail, Blain, Iverson, Kniebe, Barger, Cowie, ... 97/98/99

Cluster Lens survey

Barger etal aph/9903142

Amplification - 2.5

17 sources > 3σ

(2 mJy = 1F noise)

CUDSS

Eales,Lilly,Gear,B,...

7/98:11 sources > 3σ,

6 IDs secure,

5 faint IDs or >blank',

more area now

(1 mJy = 1σ noise)

HDF survey

Hughes etal 98

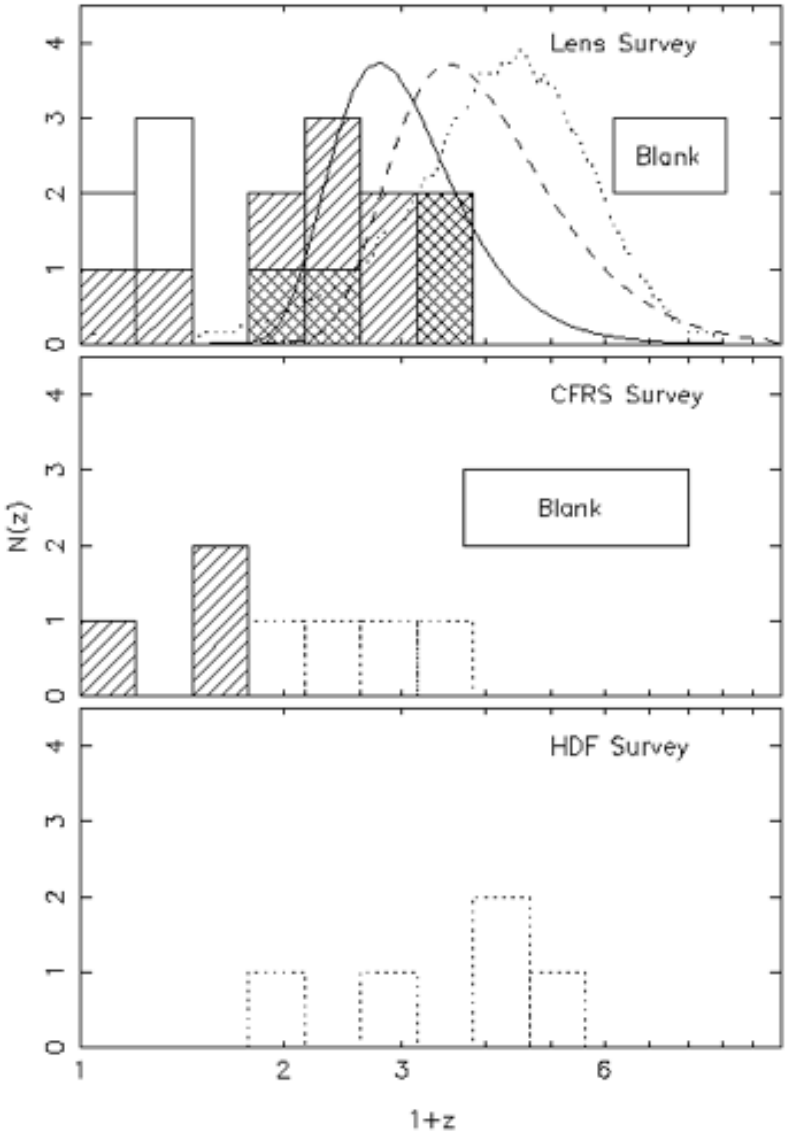

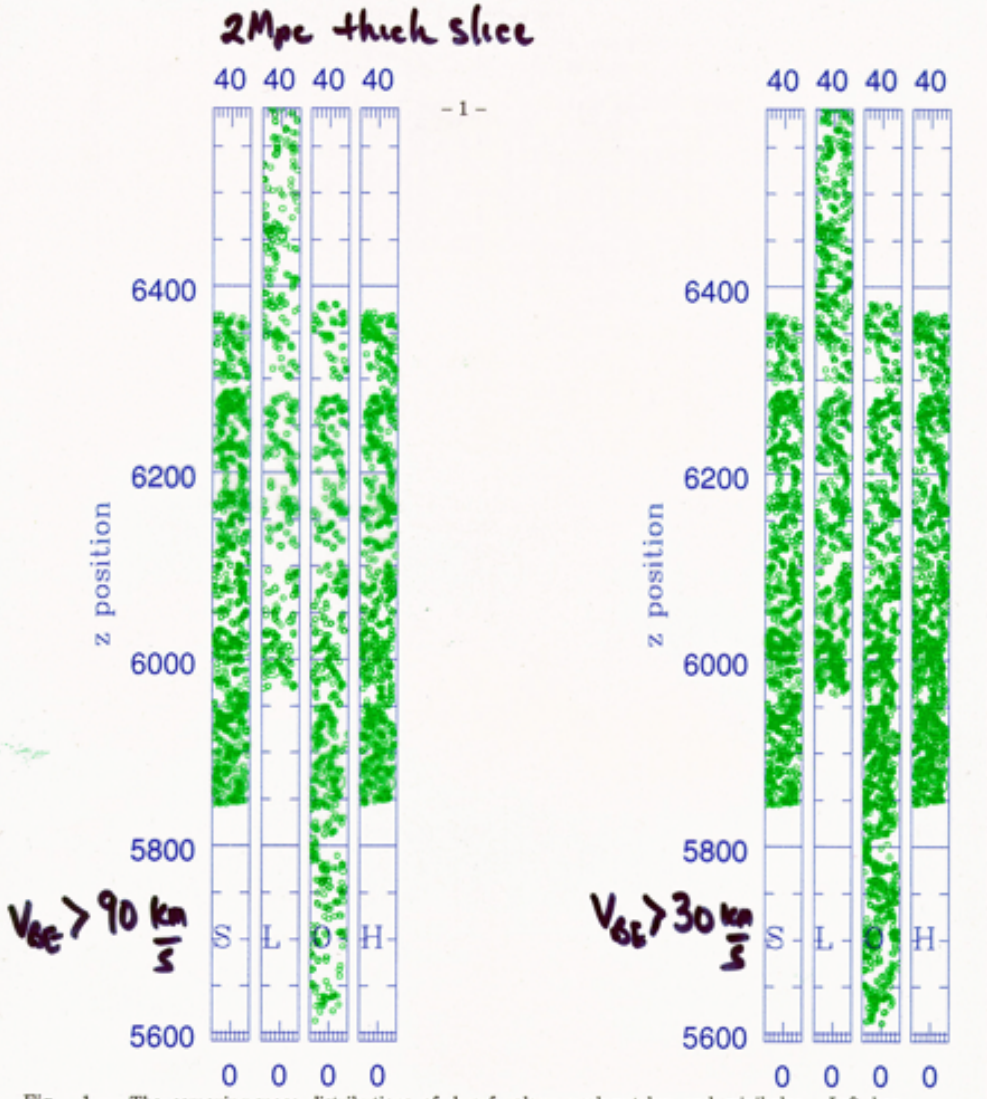

Fig. 1.— The comoving-space distributions of dwarf galaxy peak-patches and minihalos. Left has $v_{BE} > 90\,\mathrm{km\ s^{-1}}$, right has $v_{BE} > 30\,\mathrm{km\ s^{-1}}$. The slice is 2 Mpc thick, and the tiling boxes were 40 Mpc. The filaments bridging these dwarf galaxies define the lower N_{HI} Lyα forest, while halos with $v_{BE} \sim 30\,\mathrm{km\ s^{-1}}$ dominate the $N_{HI} \sim 10^{15}$ regime. The forest hydro simulations cover only 1/8 of the 40 Mpc at high resolution. This figure therefore emphasizes large scale waves must be included in our small scale "shear-patch" simulations, whose size is governed by our need to resolve 1 kpc structure in galaxies at z=3. The patches then typically include many $30\,\mathrm{km\ s^{-1}}$ halos but only a handful of $90\,\mathrm{km\ s^{-1}}$ ones. The currently largest periodic simulations with this resolution are not much bigger, but miss the long waves. We can use these peak-patch/cosmic web simulations to compare predictions for different cosmologies with the large scale structure probed by multiple quasar line-of-sight data and long range velocity space correlations in quasar spectra as well as emerging high-z catalogues.

$\frac{\delta E}{E_{cmb}}$

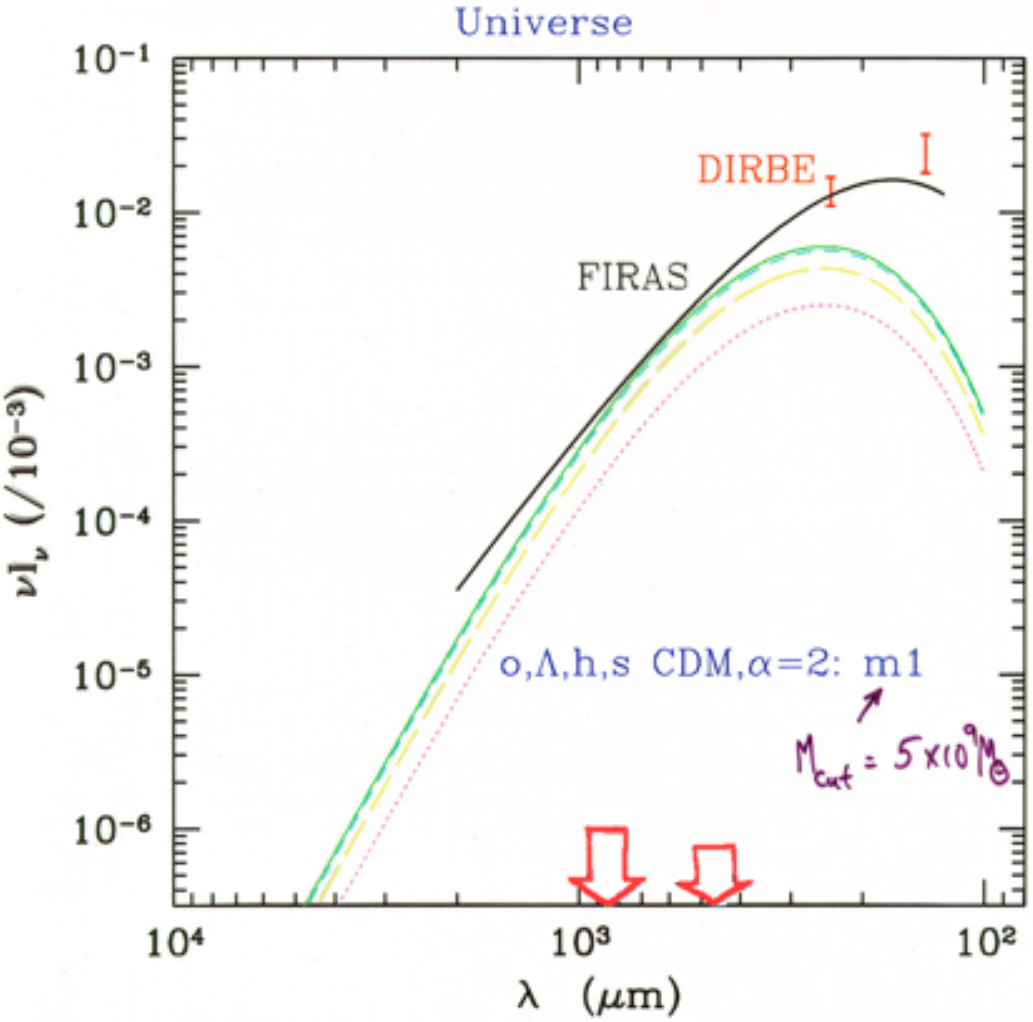

GALAXIES $z = 2.8$ to 2.5 → SCUBA on JCMT

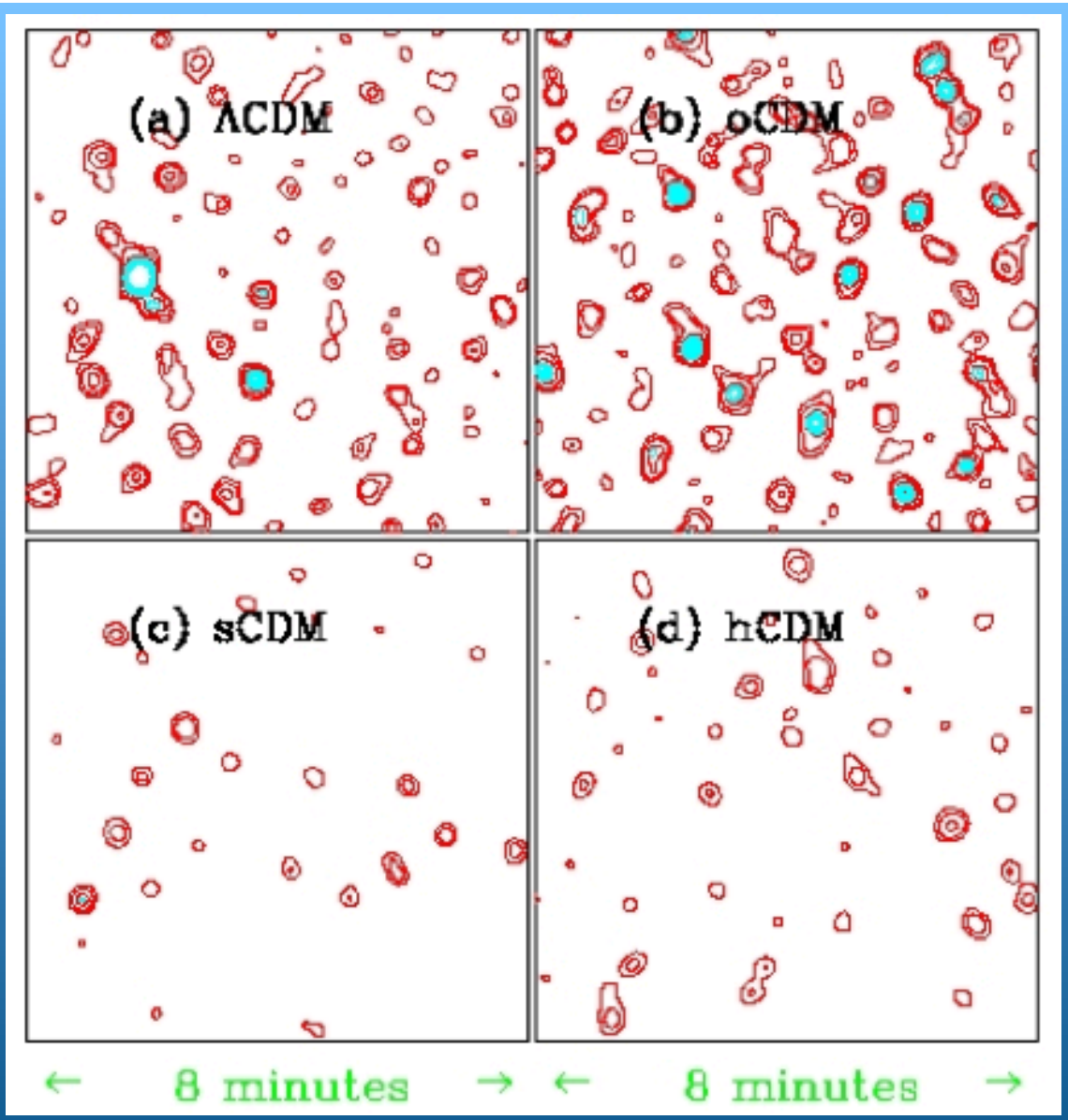

JCMT SCUBA Experiment

14" beam, 30" throw

"CHOP & WOBBLE"

CONTOUR

1/3 mJy/beam

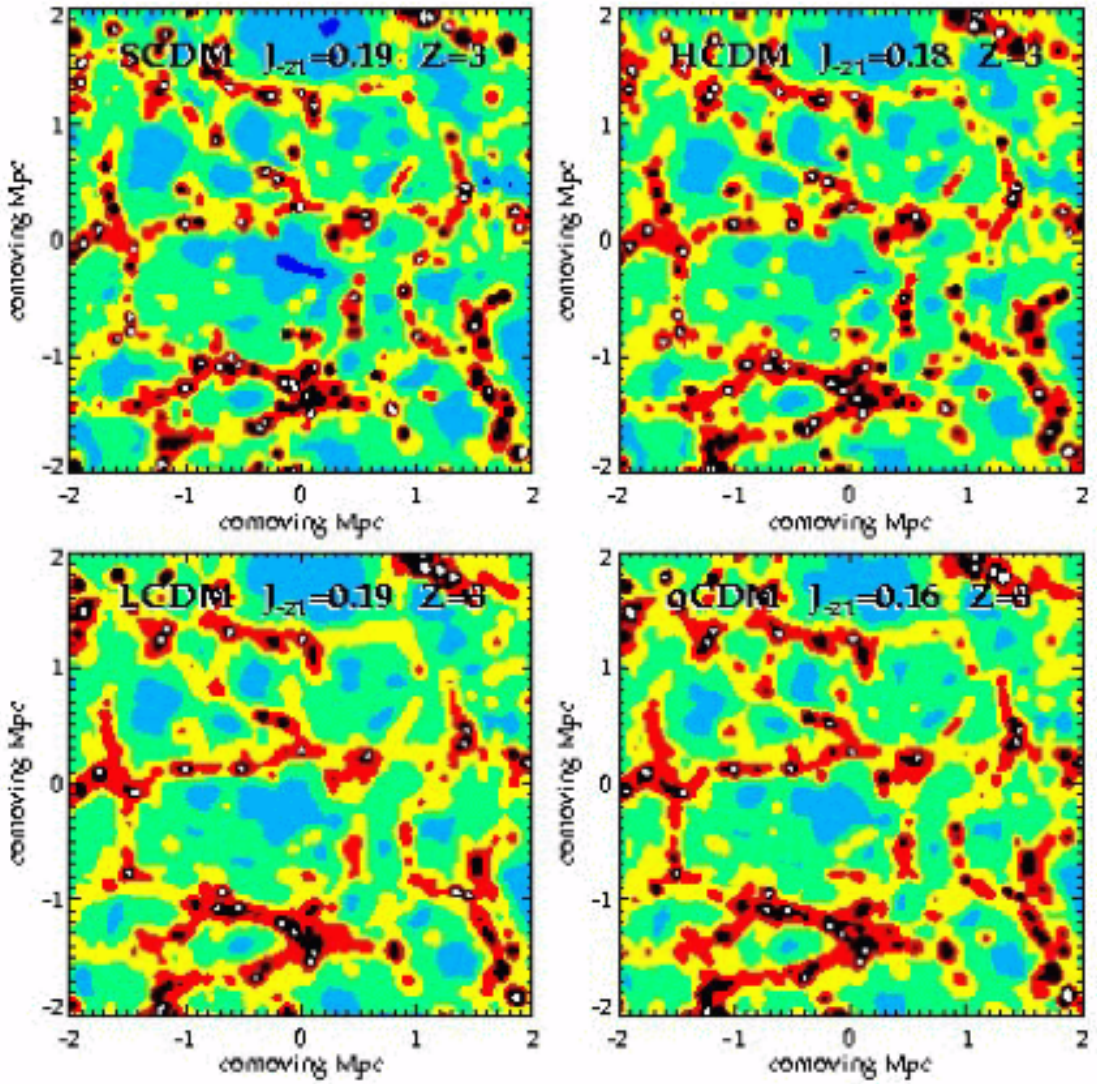

Fig. 3.— N_{HI} Column density through 2 Mpc thick slices at $z = 3$. The cosmologies shown, clock-wise from the top left are SCDM, HCDM, OCDM and ΛCDM. J_{21} has been adjusted in each case to fit the flux decrement observations of Rauch *et al.* (1997). The contours in $log_{10}N_{HI}$ are 11-12.75 (dark), 13 (dark grey), 13.5 (medium grey), 14 (light grey), 14.5 (dark), 15 (black) and 17 (white).

SIMPLE "SHELL" MODEL of NONLINEAR EVOL^N

$\Rightarrow \delta \sim 5\text{-}10_{7-}$ filaments

~ few membranes

d = 3
SPHERICAL EVOL^N

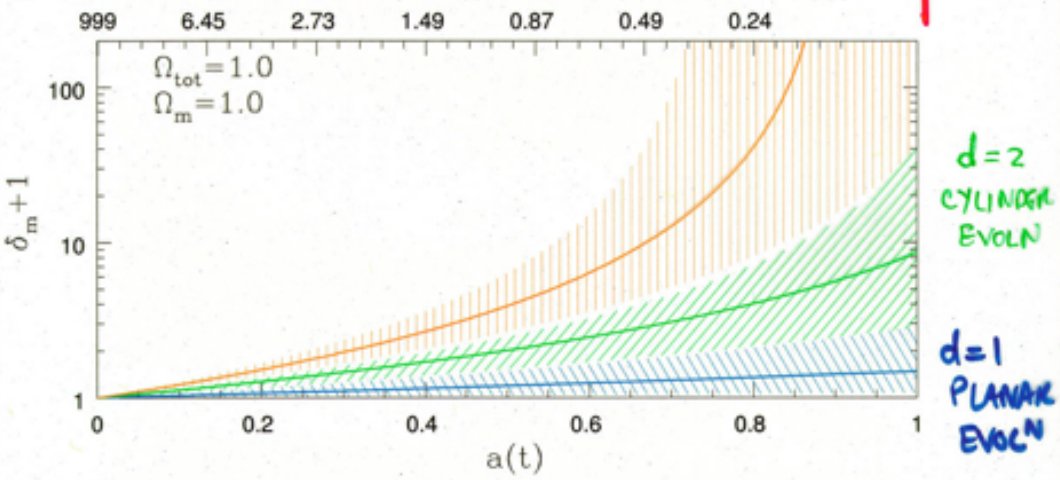

d = 2
CYLINDER EVOLN

d = 1
PLANAR EVOL^N

Fig. 7.— The nonlinear density evolution $\delta(t)$ of idealized spheres (top curve), filaments (middle) and membranes (bottom) of Lagrangian scale R_f for which the smoothed linear *rms* amplitude of density fluctuations $\sigma(R_f)$ is 0.65. Solid curves show $\delta(t)$ for the structures with initial (linear) density equal to $\bar{\delta}_d + 2\sigma_d$, $d = 1, 2, 3$. The shaded bands delineate the range of $\delta(t)$ for initial densities $[\bar{\delta}_d + \sigma_d, \bar{\delta}_d + 2.5\sigma_d]$. Values of $\bar{\delta}_d$ and σ_d are given in Fig. 3.

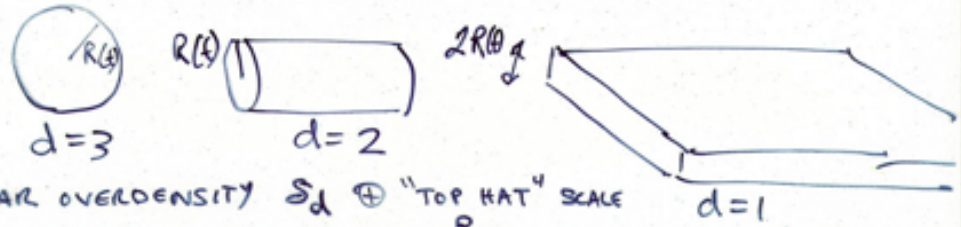

LINEAR OVERDENSITY δ_d ⊕ "TOP HAT" SCALE R_{TH}

$$\Rightarrow \ddot{R} = H_0^2 \left[\frac{(3-d)}{2d}\Omega_m + a^3\Omega_\Lambda - \frac{3}{2d}\Omega_m (1 + D(t_i)\bar{\delta}_d) \left(\frac{aR_{TH}}{R}\right)^d \right] \frac{R}{a^3}$$

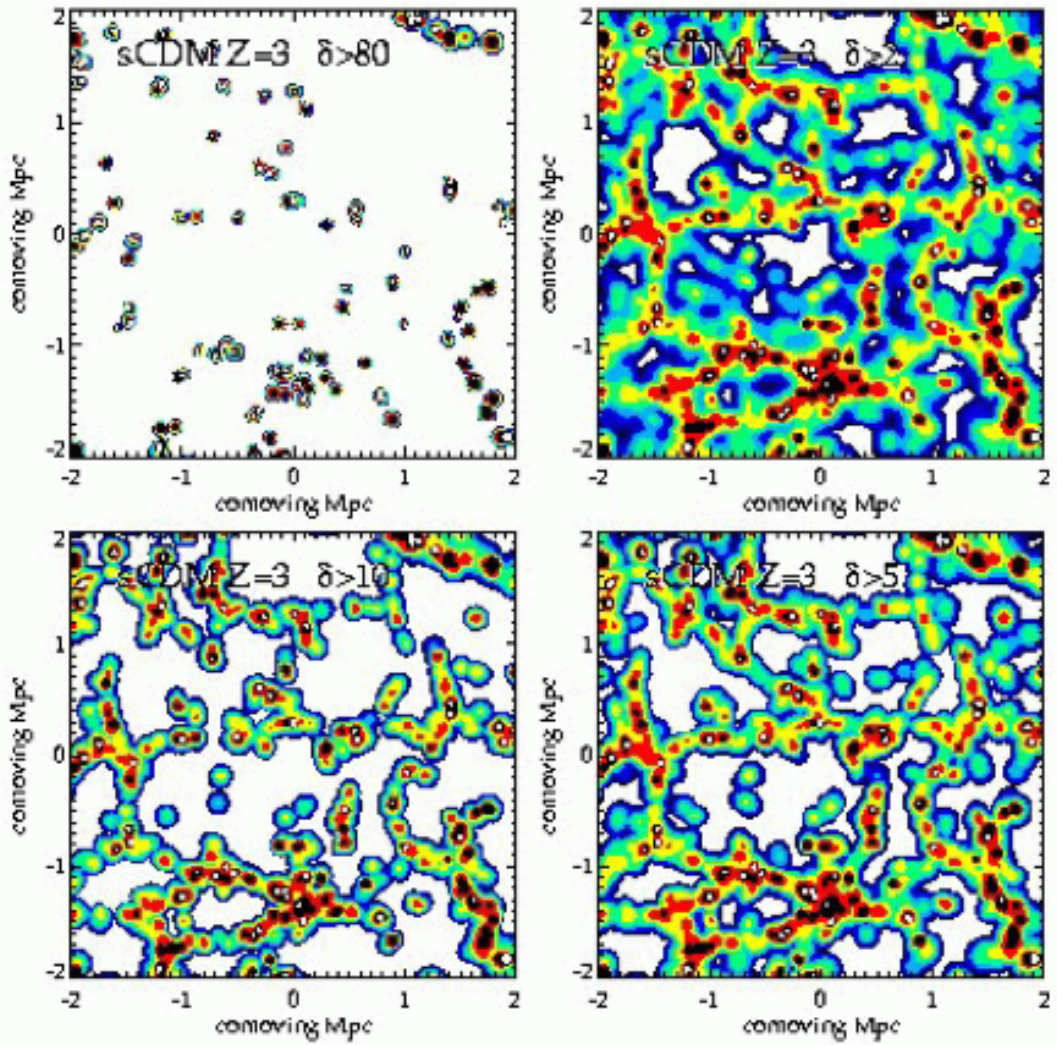

Fig. 31.— The Lyman-α intercloud medium: Column density, N_{HI}, through 2 Mpc thick slices for four cosmologies with UV flux scaled to fit the observed flux decrement one-point distribution function. $\Omega_b\, h^2$=0.0125 throughout. Top left: SCDM $\nu = 0$ run, z=3 with only the $\delta > 80$ cloud contribution shown. Top right: at $\delta > 2$, the intrafilament webbing appears. The web theory of filaments predicts that the typical smoothed overdensity should be $\sim 5 - 10$. Bottom right: $\delta > 10$ gas. Bottom left: $\delta > 5$ gas. A similar story holds for other cosmologies. The contours in $log_{10} N_{HI}$ are 11-12.75 (dark), 13 (dark grey), 13.5 (medium grey), 14 (light grey), 14.5 (dark), 15 (black) and 17 (white).

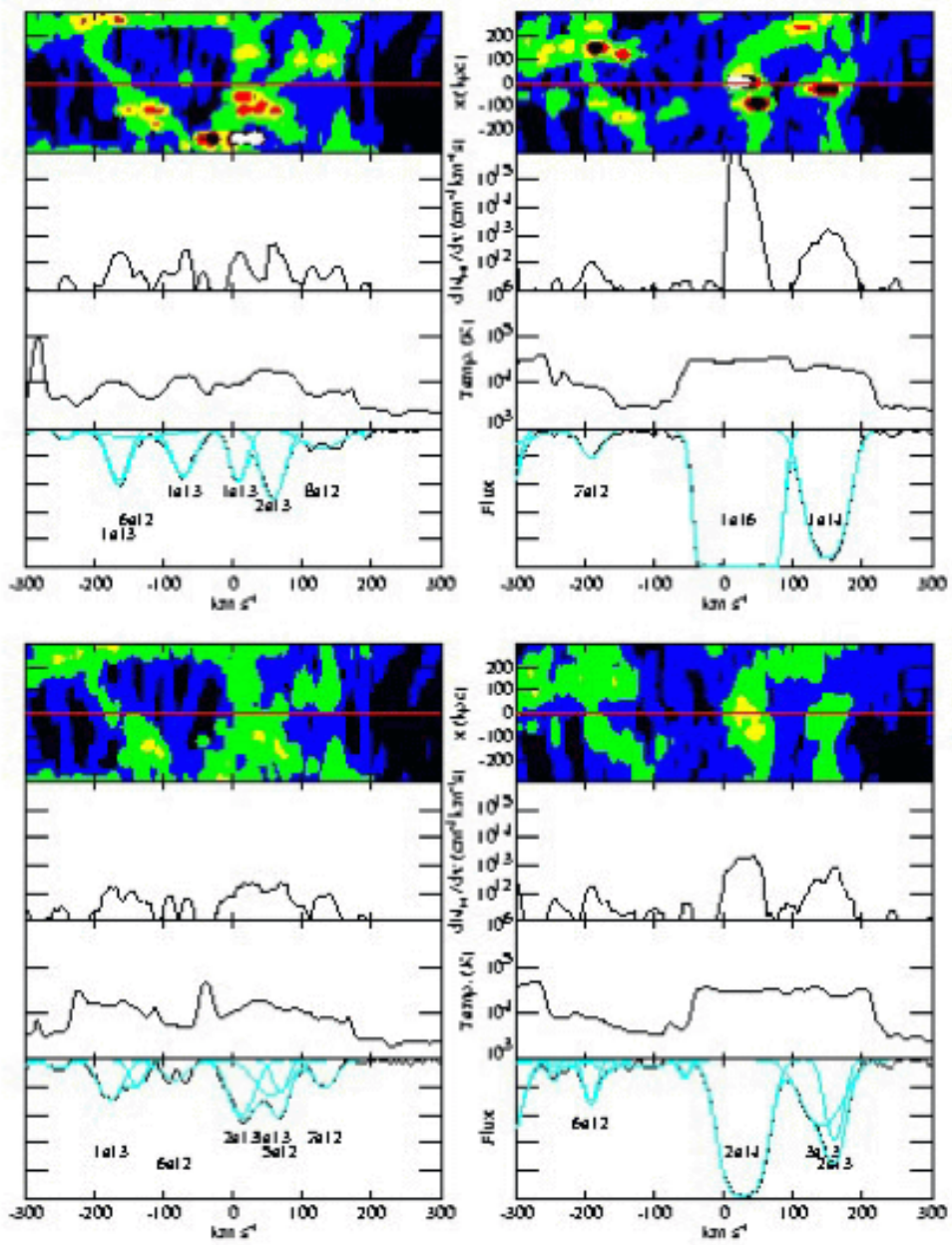

Fig. 27.— A sample line through the $\nu = 0$ CDM simulation at $z = 3$. These two figure compares the same line of sight through simulations with different resolution. This clearly shows how insufficient resolution is incapable of correctly resolving the filaments that give rise to Lyman-α absorption.

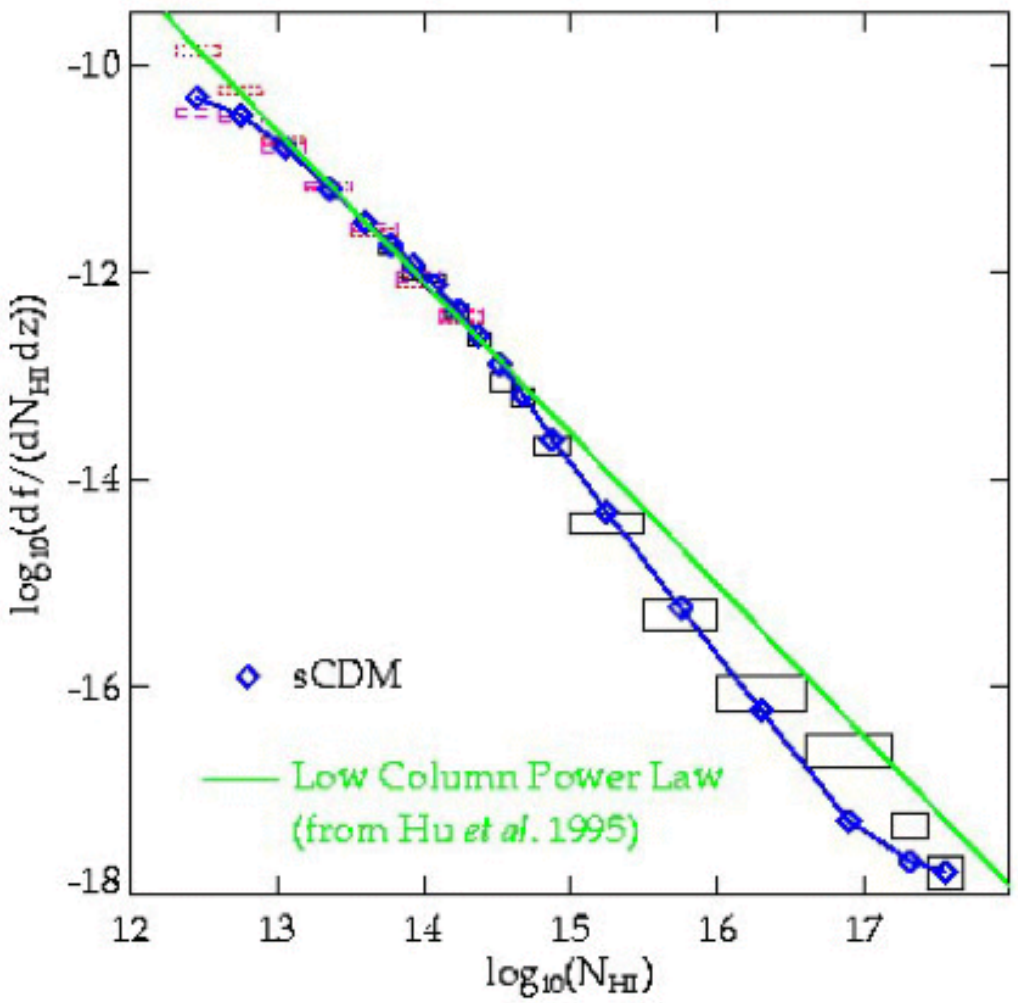

Fig. 11.— Column density distribution for our total simulations sample, $z = 3$. The plot covers 10 orders of magnitude and compares the SCDM result to the data of Petitjean *et al.* (1993) (black boxes) and Hu *et al.* (1995) (dotted and dashed boxes) ($z_{abs} \sim 2.7$). The boxes represent bins with the top and bottom of each box being the Poisson error. The dotted Hu *et al.* boxes have had a blending correction applied which has not been attempted with the simulated lines. We have adjusted the UV flux in order to fit the observed flux decrement 1 point distribution. The simulation fails to reproduce numbers of clouds above 10^{16} correctly because of self-shielding of the ionizing flux at high columns.

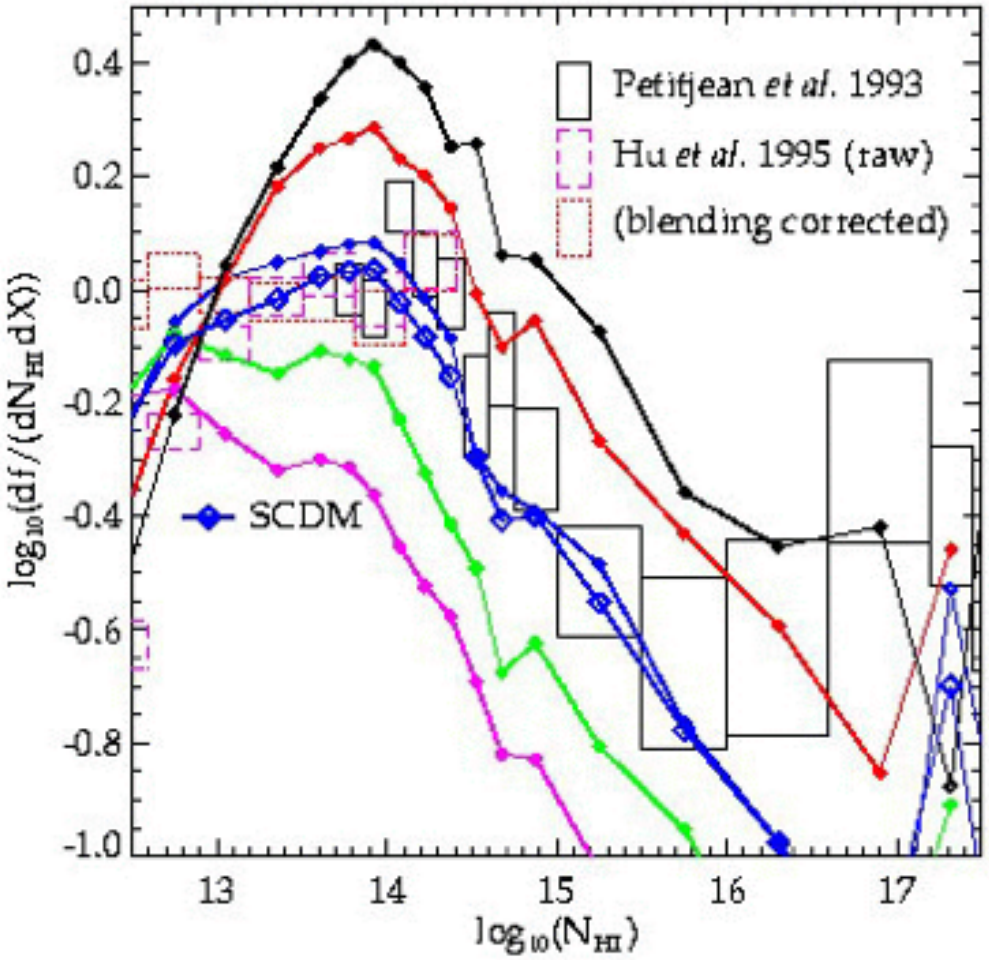

Fig. 7.— The N_{HI} Column density distribution obtained with different mean shear (ν). Five simulations with $\nu = -1.4, -0.7, 0, +0.7$ and 1.4 (curves from bottom to top) contribute to the total sample for each cosmology (connected diamond curve). The cosmology shown here is SCDM. The boxes are one sigma error regions for observed data and the lines.

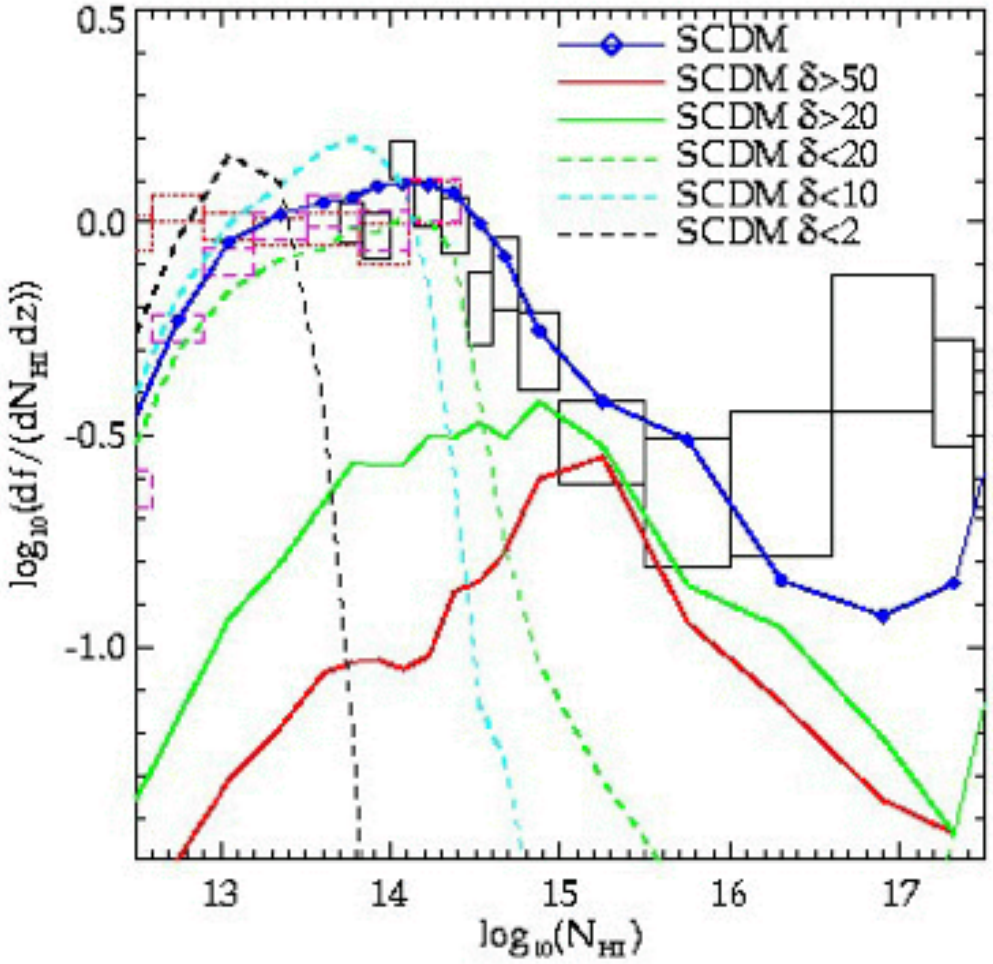

Fig. 32.— cloud/intercloud split in columns. The Column density distribution per unit redshift at $z = 3$. The observational data are plotted as boxes with widths equal to the bin widths and top and bottom edges at the positions of the 1 σ poisson error bars.

"Galaxy" peak-patch simulation

40 Mpc box (comoving)

20 Mpc region

pks at Z=4

"Galaxy" sph/P^{3}MG simulation

5 Mpc region

tidally-oriented peaks/voids overlaid

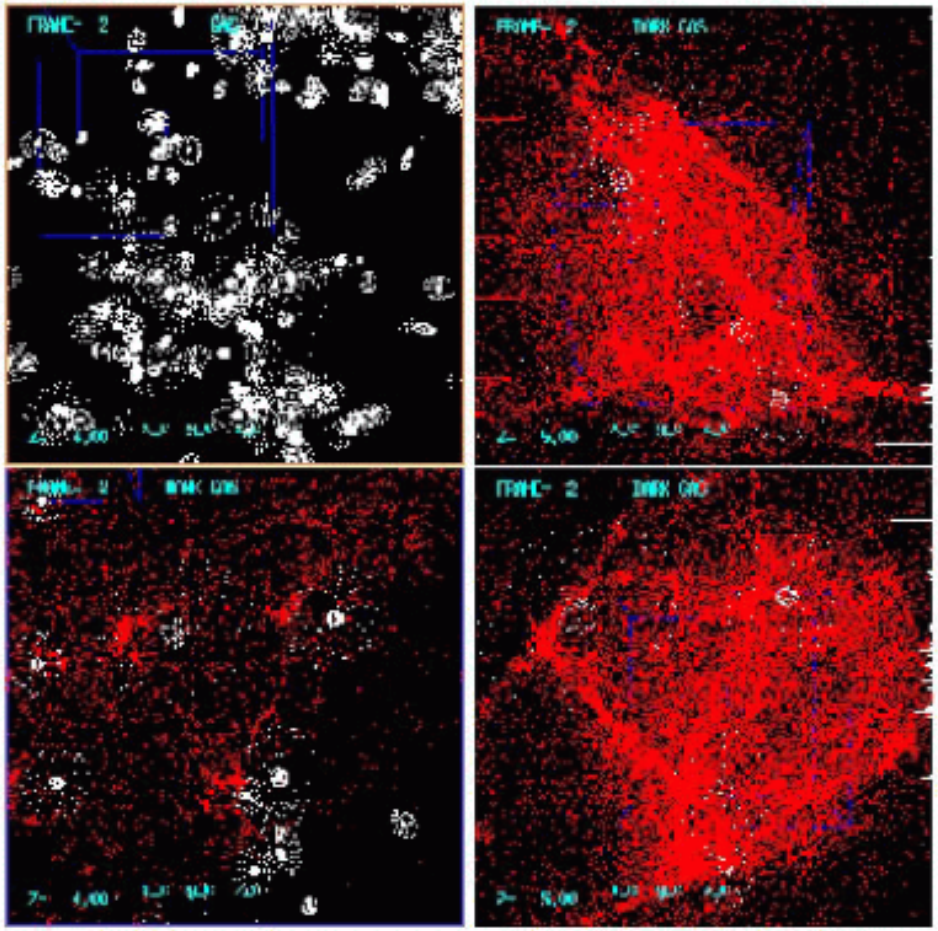

Fig. 8.— These plots show the reconstruction of a galaxy-galaxy filament present in our 40 Mpc "galaxy" simulation. The cosmology is a standard, initially scale-invariant Ω_m=1 CDM model with Ω_B=0.05, h=0.5, normalized to σ_8=0.67. We used the cosmological SPH+P^{3}MultiGrid code. We identified the peak-patches that should collapse by $z = 4$ in the initial conditions (IC), as shown in the top left panel (which is $10h^{-1}$Mpc across, comoving). For each patch, the outer ellipsoid represents the alignment of the shear tensor and the inner sphere is an estimate of the final object size. In the lower left panel, we zoom in on the central filamentary web structure and overlay dark matter from a simulation of these IC (panel $2.5h^{-1}$Mpc across). The five peak patches (at $z = 4$ with overdensity 180) and two voids that define this region were used as constraints for a new higher resolution IC (12.8 Mpc), which we also evolved numerically. These peaks are shown overlaid with dark matter from the new simulation in the right hand panels. The top right panel is a different orientation to the others that shows the filament more clearly, also shown in n_{yy} in figure 9. These panels demonstrate that peaks represent an excellent way to compress the essential information about large scale filamentary behaviour.

"Ly alpha" filament simulation

5 Mpc region

reconstruct IC

7peak/2void constraint

5 Mpc diam

high res core

5 Mpc comoving

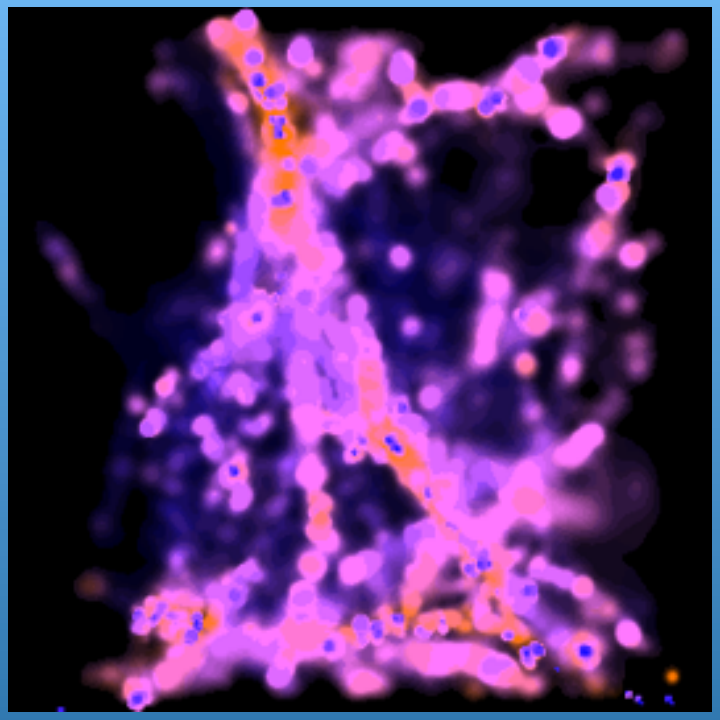

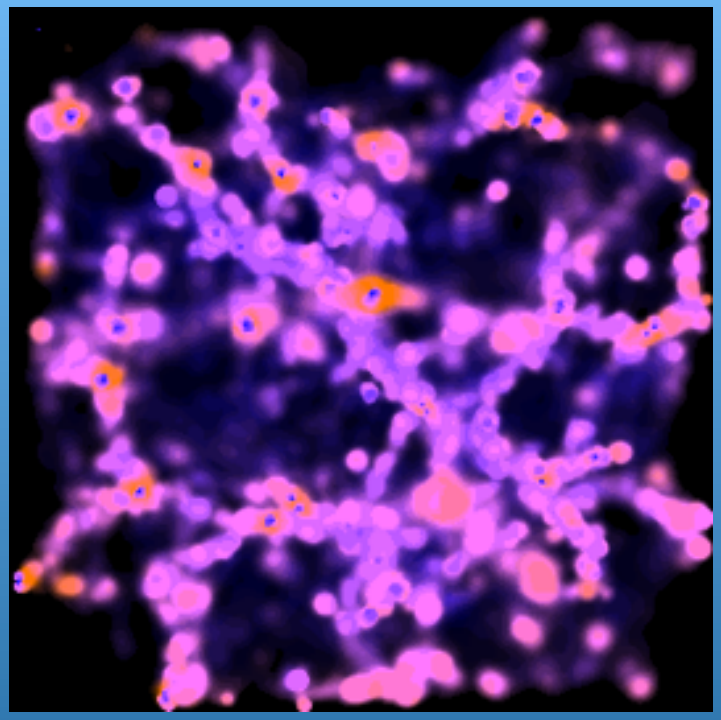

Z=4

CONSTRAINED
"FILAMENT" PATCH

Via a 5-peak 2-void
dwarf galaxy constraint

Z=3

AMBIENT
"SHEARING" PATCH

$< \delta_L >_{1Mpc} = 0$, "$v_b = 0$"

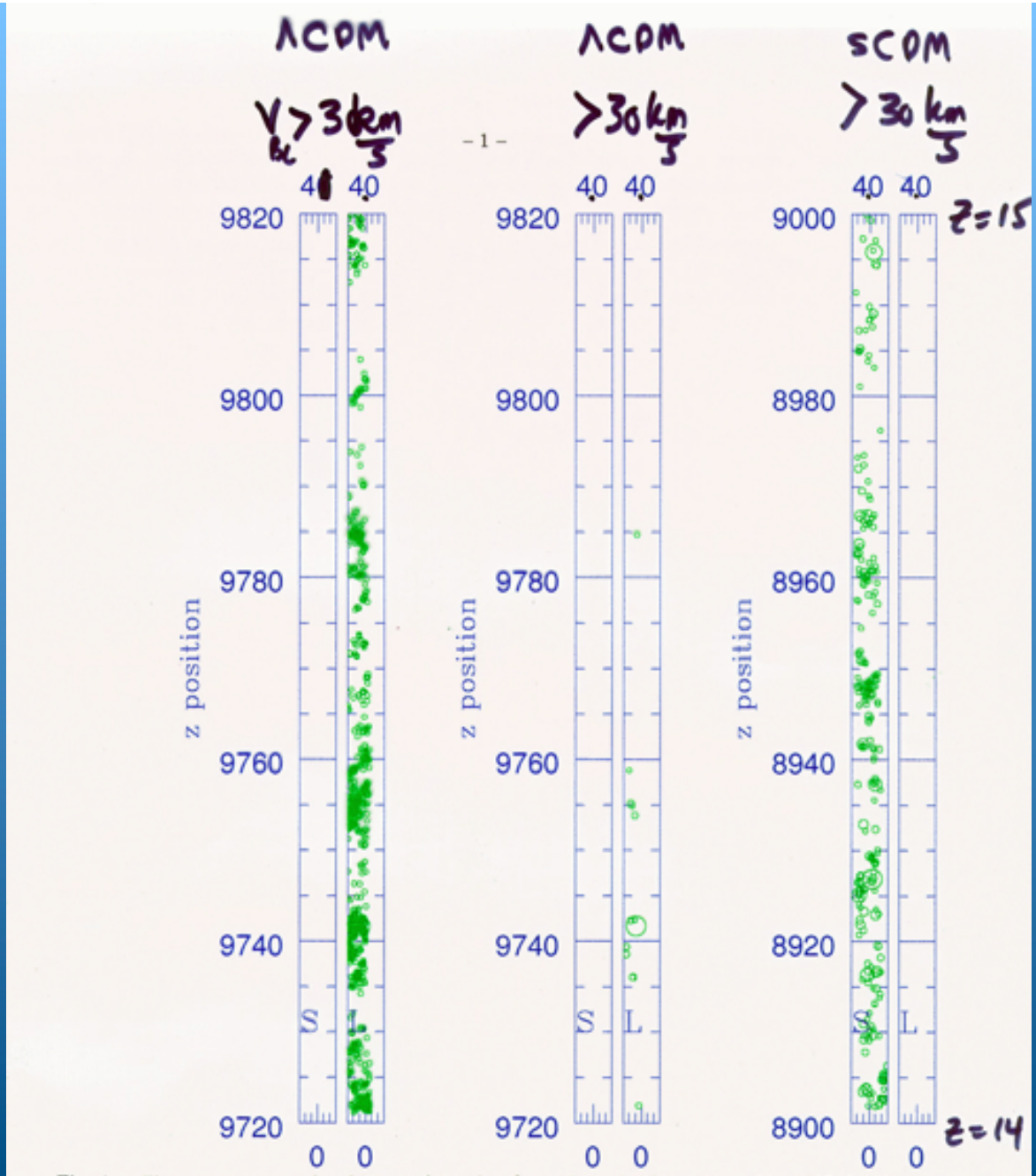

Fig. 1.— The comoving-space distributions of tiny dwarflet peak-patches between $z = 14$ and 15. Left has $v_{BE} > 3\,\mathrm{km\ s^{-1}}$, middle and right have $v_{BE} > 30\,\mathrm{km\ s^{-1}}$. The tiling boxes were 4 Mpc.

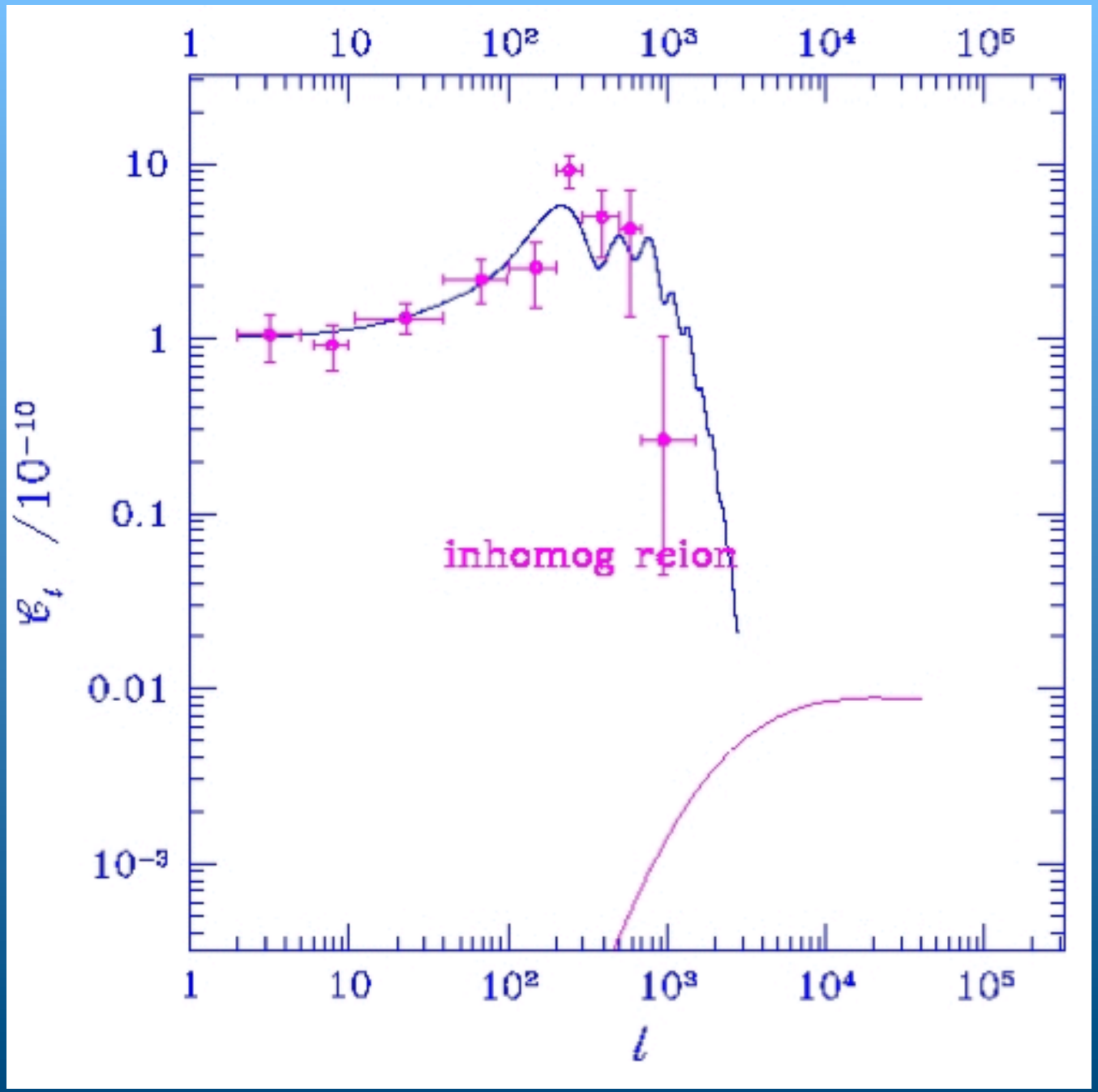

Knox
Scoccimarro
Dodelson

astro ph/
9805012

$P(\text{sign} \mid \frac{\delta}{\sigma})$ $P(\frac{\delta}{\sigma} \mid \text{sign})$

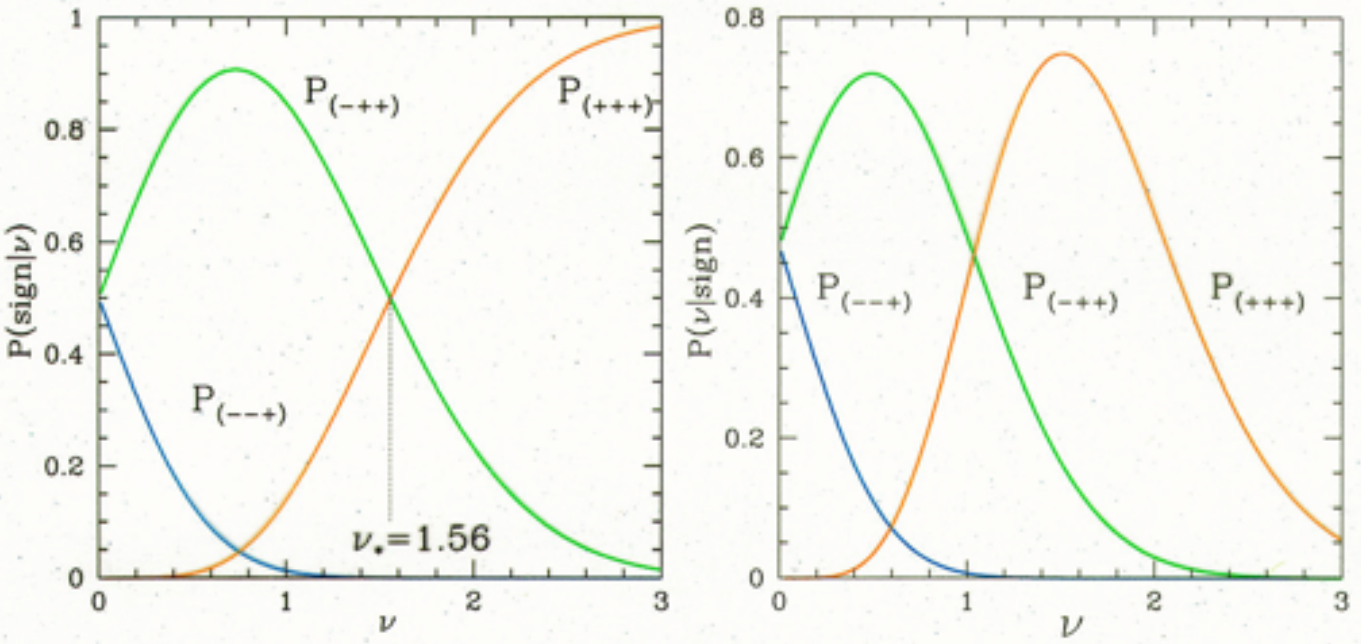

Fig. 6.— Left panel: Probablity of the eigenvalue signature given the overdensity threshold $P(\text{sign}|\nu)$, $\nu = \delta/\sigma$. Right panel: Density distribution given the type of shear tensor, $P(\nu|\text{sign})$. Mean densities for the given shear type are $\bar{\delta}_d \approx 1.66\sigma, 0.6\sigma, -0.6\sigma$ for $(+++),(-++)$ and $(--+)$ cases labeled by $d = 3, 2, 1$ with dispersion $\sigma_d \approx 0.55\sigma$ almost equal for all configurations.

$\Rightarrow$ Sub-M_* more filamentary

RESOLUTION - SMOOTHED MAP $X_{b,i} = r_i - S_{b,i}(r,t)$

$\sigma_p \lesssim 1.7$

$\partial^2\bar{\Phi}/\partial r_i \partial r_j$

DEFORMATION TENSOR (∝ TIDAL TENSOR)

$$e_{b,ij} = -\frac{1}{2}\left(\frac{\partial S_{b,i}}{\partial r_j} + \frac{\partial S_{b,j}}{\partial r_i}\right) = -\sum \lambda_A \hat{n}^i_A \hat{n}^j_A$$

$\lambda_3 \geq \lambda_2 \geq \lambda_1$ CONVENTION

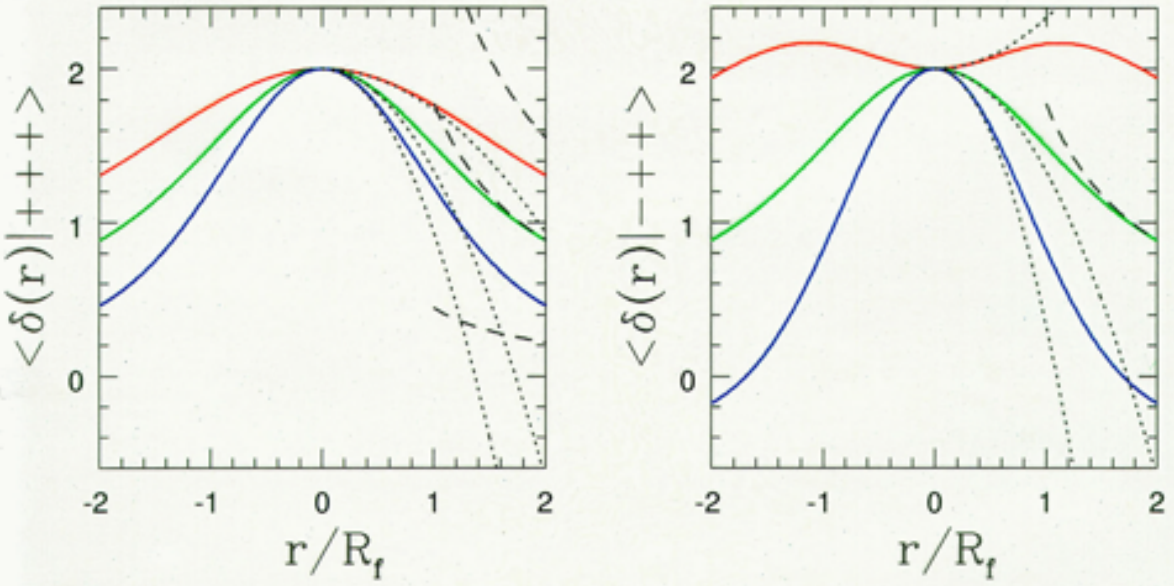

Fig. 4.— Constrained primordial density field $\langle\delta(\mathbf{r})|\lambda_1,\lambda_2,\lambda_3\rangle$ as a function of distance r in units of the filter scale R_f, in the three eigendirections (1-top, 3-bottom). The left plot corresponds to the shear with all positive (+++) eigenvalues. The right plot represents the case of "filamentary" behaviour of the density in the neighbourhood of the (−++) sheared point. Dotted and dashed curves show the analytic short and long distance asymptotics .

One negatwe evalue, 2 positive
⇒ filament tendency .

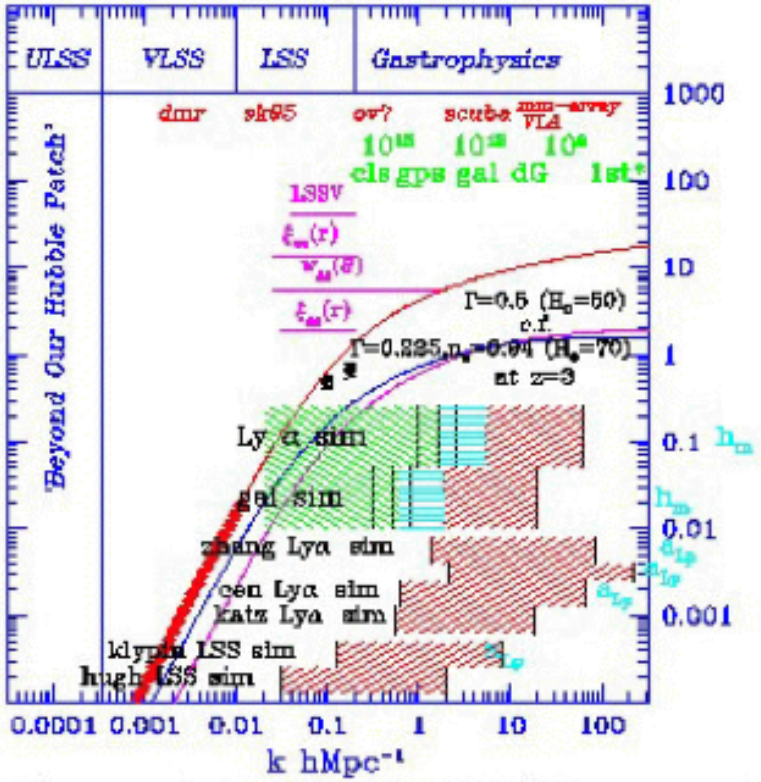

Fig. 3.— The two (linear) power spectra shown (scaled to redshift 3) The upper curve at high k is the standard untilted CDM model, but normalized to cluster abundances, $\sigma_8 = 0.67$. The other has the same cosmological age (13 Gyr) and $\Omega_B h^2$ (0.0125) but $H_0 = 70$ with $\Omega_\Lambda = 0.67$, slightly tilted to be COBE-normalized ($n_s = 0.91$). (Also shown is a COBE-normalized CDM model, which misses the solid data point in the cluster-band (constraint from dn_{cl}/dT_x).) The bands in comoving wavenumber probed by various simulations are contrasted. Periodic simulations may use the entire volume, but the k-space restriction to lie between the fundamental mode (low-k boundary line) and the Nyquist wavenumber (high-k boundary line) in the IC can severely curtail the rare events in the medium that observations especially probe, and prevents tidal distortions of the simulation volume. We use 3 k-space sampling procedures (FFT and two direct PIs) with the boundaries defined by which has the smallest volume per k-mode. Even though a 256^3 Fourier transform was used, notice how early the direct sampling takes over (with only 10000 modes). Using an FFT with the very flat spectra in the dwarf galaxy (dG) band can give misleading results. The 3 low-k lines shown for our Lyα and galaxy simulations correspond to the high, medium and low resolution fundamental modes. We actually include modes in the entire hatched region, with the tidal fields associated with the longer waves included by a self-consistent uniform tide on the LR simulation volume. k_m denotes our best resolution. a_{L_0} denotes the physical (best) lattice spacing for the grid-based Eulerian hydro codes of Cen and Zhang *et.al.* ($z = 3$). k-space domains for two large scale structure ($z = 0$) simulations are also shown, a Klypin 256^3 PM calculation and a Couchman (labelled *hugh*) 128^3 P^3M simulation.